



eCOMMONS

Loyola University Chicago  
Loyola eCommons

---

Master's Theses

Theses and Dissertations

---


1993

## Electrochemical Studies of Swelling and Shrinking of Clay Films

Jia Du

Loyola University Chicago

Follow this and additional works at: [https://ecommons.luc.edu/luc\\_theses](https://ecommons.luc.edu/luc_theses)

 Part of the [Chemistry Commons](#)

---

### Recommended Citation

Du, Jia, "Electrochemical Studies of Swelling and Shrinking of Clay Films" (1993). *Master's Theses*. 3927.  
[https://ecommons.luc.edu/luc\\_theses/3927](https://ecommons.luc.edu/luc_theses/3927)

This Thesis is brought to you for free and open access by the Theses and Dissertations at Loyola eCommons. It has been accepted for inclusion in Master's Theses by an authorized administrator of Loyola eCommons. For more information, please contact [ecommons@luc.edu](mailto:ecommons@luc.edu).



This work is licensed under a [Creative Commons Attribution-Noncommercial-No Derivative Works 3.0 License](#).  
Copyright © 1993 Jia Du

**LOYOLA UNIVERSITY OF CHICAGO**

**ELECTROCHEMICAL STUDIES  
OF SWELLING AND SHRINKING OF CLAY FILMS**

**A THESIS SUBMITTED TO  
THE FACULTY OF THE GRADUATE SCHOOL  
IN CANDIDACY FOR THE DEGREE OF  
MASTER OF SCIENCE**

**DEPARTMENT OF CHEMISTRY**

**BY**

**JIA DU**

**CHICAGO, ILLINOIS**

**January 1993**

**Copyright by Jia Du**  
**September, 1992**  
**All Rights Reserved**

## **ACKNOWLEDGEMENTS**

I would like to express my deep appreciation to Professor Alanah Fitch for her direction and encouragement in the carrying out of this work, her willingness to help at any time, her moral and financial support throughout this study and especially for her great patience.

Special thanks are due to the members of my committee, Professors Albert Herlinger, David Crumrine, and Ken Olsen for taking time to read my thesis, and for their helpful suggestions during the course of this work.

My lab colleagues Jennifer Stein, Sam Lee, Qinfen Rong, and Dr. Subramanian earned my considerable debt as did Mr. Joe Schluep of Biology Department for SEM help, the staff in the Chemistry Department, all my fellow graduate students and the faculty for their generosity and constructive criticisms. I would also like to acknowledge the Graduate School for their financial support.

I appreciate the great support, encouragement, and friendship from many people such as Bob Bernat, Zhong-Min Lu etc.

Finally, I would like to thank my family: my wife for picking me up when I was down, my parents and my brother for their support throughout my academic career, and my parents-in-law for their distant encouragement.

# TABLE OF CONTENTS

	<b>Page</b>
<b>ACKNOWLEDGEMENTS</b>	iii
<b>LIST OF PUBLICATIONS</b>	vii
<b>LIST OF TABLES</b>	viii
<b>LIST OF FIGURES</b>	ix
<b>LIST OF ABBREVIATIONS</b>	xi
<b>CHAPTER</b>	
<b>I. INTRODUCTION</b>	<b>1</b>
I. Statement of the Problem	1
II. Clay Chemistry Background	1
III. Goal of Clay Chemistry Study	7
IV. Technique: Cyclic Voltammetry (CV)	7
V. Synopsis of Experiments	11
<b>II. EXPERIMENTAL METHOD</b>	<b>14</b>
<b>I. Experimental</b>	<b>14</b>
<b>I.1. General Methods</b>	<b>14</b>
I.1.1. Instruments	14
I.1.2. Chemicals and Clay Samples	15
<b>II. Procedures</b>	<b>15</b>
II.1.1. Clay Sample Purification	15
II.1.2. Preparation of the Analyte	16

II.1.3.	Preparation of Supporting Electrolyte	17
II.1.4.	Electrochemical Experimental Setup	17
II.1.5.	Procedures of Cleaning the Pt Electrode	24
II.1.6.	Spin-Coating Clay Modified Electrode (SPCME) Fabrication	24
II.1.7.	Cyclic Voltammetric Scans in Both Electrolyte Background and in the Analyte Solution	25
<b>III.</b>	<b>Pt Working Electrode Characterization</b>	<b>25</b>
<b>IV.</b>	<b>Studies on SWy-1 Clay</b>	<b>26</b>
IV.1.1.	Scanning Electron Microscopy (SEM)	26
IV.1.2.	SPCME Stability	27
IV.1.3.	Effect of Scan Rate on the CME Diffusion Layer	27
IV.1.4.	Effect of NaCl Concentration on the Swelling of SWy-1 Clay	28
IV.1.5.	Comparison Between $\text{Na}_3[\text{Fe}(\text{CN})_6]$ Probe and $\text{K}_3[\text{Fe}(\text{CN})_6]$ Probe	28
IV.1.6.	Comparison Between $\text{Na}_4[\text{Fe}(\text{CN})_6]$ Probe and $\text{Na}_3[\text{Fe}(\text{CN})_6]$ Probe	29
IV.1.7.	Effect of NaCl Concentration on SWy-1 (reduced form)	29
<b>V.</b>	<b>Studies on SAz-1 Clay</b>	<b>29</b>
V.1.1.	Effect of NaCl Concentration on the Swelling of SAz-1 ( $\text{Ca}^{2+}$ form)	29
V.1.2.	Effect of KCl Concentration on the Swelling of SAz-1 ( $\text{Ca}^{2+}$ form)	30
V.1.3.	Effect of $\text{CaCl}_2$ Concentration on the Swelling of SAz-1 ( $\text{Ca}^{2+}$ form)	30

V.1.4.	Effect of NaCl Concentration on the Swelling of SAz-1 (Na <sup>+</sup> -exchanged form)	30
V.1.5.	Effect of KCl Concentration on the Swelling of SAz-1 (Na <sup>+</sup> -exchanged form)	31
<b>III.</b>	<b>RESULTS AND DISCUSSION</b>	<b>32</b>
<b>I.</b>	<b>Pt Working Electrode Characterization</b>	<b>32</b>
<b>II.</b>	<b>Studies on SWy-1 Clay</b>	<b>32</b>
1.	Scanning Electron Microscopy (SEM)	32
2.	SPCME Stability	36
3.	Effect of Scan Rate on the CME Diffusion Layer	44
4.	Effect of NaCl Concentration on the Swelling of SWy-1 Clay	56
5.	Comparison among Na <sub>3</sub> [Fe(CN) <sub>6</sub> ], Na <sub>4</sub> [Fe(CN) <sub>6</sub> ] Probe and Na <sub>3</sub> [Fe(CN) <sub>6</sub> ] Probe	58
6.	Effect of NaCl Concentration on SWy-1 (reduced form)	64
<b>III.</b>	<b>Studies on SAz-1 Clay</b>	<b>64</b>
1.	Effect of NaCl, KCl and CaCl <sub>2</sub> Concentration on the Swelling of SAz-1 (Ca <sup>2+</sup> -form)	64
2.	Effect of NaCl and KCl Concentration on the Swelling of SAz-1 (Na <sup>+</sup> -exchanged form)	75
<b>IV.</b>	<b>Summary and Future Direction</b>	<b>81</b>
	<b>Bibliography</b>	<b>84</b>
	<b>VITA</b>	<b>88</b>

## LIST OF PUBLICATIONS

Fitch, A. and Du, J.; *J. Electroanal. Chem.*, **1991**, 319, pp. 409-414.



## LIST OF TABLES

Tables		Page
1.	SWy-1 and SAz-1 Clay Data	4
2.	NaCl solution preparation	18
3.	KCl solution preparation	20
4.	CaCl <sub>2</sub> solution preparation	22
5.	Pt working electrode characterization experiment results	33
6.	SPCME stability experiment results	43
7.	Scan rate dependence of the maximum cathodic current for 4 mM K <sub>3</sub> [Fe(CN) <sub>6</sub> ] in 2 M and 0.02 M NaCl at 25 μg SWy-1 SPCME	55
8.	NaCl effect on SWy-1 clay	57
9.	Effects of Na <sub>3</sub> [Fe(CN) <sub>6</sub> ] and Na <sub>4</sub> [Fe(CN) <sub>6</sub> ] probes	63
10.	[NaCl] effect on reduced SWy-1	67
11.	[NaCl], [KCl], [CaCl <sub>2</sub> ] effect on SAz-1	74
12.	[NaCl], [KCl] effect on SAz-1 (Na <sup>+</sup> -exchanged form)	80

## LIST OF FIGURES

FIGURES	Page
1. A display of typical cyclic voltammogram.	10
2. A plot of the cathodic current vs. square root of scan rate for 4 mM $K_3[Fe(CN)_6]$ , 0.7 M NaCl.	35
3. SEM image of 1 $\mu$ l SWy-1 spin-coated film from top topography.	38
4. SEM image of 1 $\mu$ l SWy-1 spin-coated film viewing from the back side of the film.	40
5. A plot of the ratio of $i_{pc}$ over $i_{bare}$ vs. soaking time for 4 mM $K_3[Fe(CN)_6]$ .	42
6. Maximum current obtained as a function of the scan rate for SWy-1 spin-coated Pt electrodes.	46
7. Maximum current obtained as a function of the scan rate for SAz-1 spin-coated Pt electrodes in 2 M NaCl.	48
8. Scan rate dependence of the maximum cathodic current for 4 mM $K_3[Fe(CN)_6]$ in 2 M and 0.02 M NaCl at 25 $\mu$ g spin-coated SWy-1 modified electrode.	52
9. A plot of the ratio of $i_{pc}$ over $i_{bare}$ vs. 1/SQRT[NaCl] for 4 mM $[Fe(CN)_6]^{3-}$ for 1 $\mu$ l of 35 g/l SWy-1 SPCME.	54
10. A plot of ratio ( $i_{pcme}/i_{bare}$ ) vs. 1/SQRT[NaCl] obtained for 4 mM $Na_3[Fe(CN)_6]$ probe at 1 $\mu$ l 35 g/l SWy-1 SPCME.	60
11. A plot of ratio ( $i_{pcme}/i_{bare}$ ) vs. 1/SQRT[NaCl] obtained for 4 mM $Na_4[Fe(CN)_6]$ probe at 1 $\mu$ l 35 g/l SWy-1 SPCME.	62
12. A plot of ratio vs. 1/SQRT[NaCl] obtained for 4 mM $K_3[Fe(CN)_6]$ at 1 $\mu$ l 35 g/l reduced SWy-1 SPCME.	66

13. A plot of ratio vs.  $1/\text{SQRT}[\text{NaCl}]$  obtained at  $1 \mu\text{l}$  35 g/l SAz-1 SPCME for 4 mM  $\text{K}_3[\text{Fe}(\text{CN})_6]$ . 69
14. A plot of ratio vs.  $1/\text{SQRT}[\text{KCl}]$  obtained at  $1 \mu\text{l}$  35 g/l SAz-1 SPCME for 4 mM  $\text{K}_3[\text{Fe}(\text{CN})_6]$  probe. 71
15. A plot of ratio vs.  $1/\text{SQRT}[\text{CaCl}_2]$  obtained at  $1 \mu\text{l}$  35 g/l SAz-1 SPCME for 4 mM  $\text{K}_3[\text{Fe}(\text{CN})_6]$  probe. 73
16. A plot of ratio vs.  $1/\text{SQRT}[\text{NaCl}]$  obtained at  $1 \mu\text{l}$  35 g/l SAz-1 ( $\text{Na}^+$ -exchanged form) SPCME for 4 mM  $\text{K}_3[\text{Fe}(\text{CN})_6]$  probe. 77
17. A plot of ratio vs.  $1/\text{SQRT}[\text{KCl}]$  obtained at  $1 \mu\text{l}$  35 g/l SAz-1 ( $\text{Na}^+$ -exchanged form) SPCME for 4 mM  $\text{K}_3[\text{Fe}(\text{CN})_6]$  probe. 79

## LIST OF ABBREVIATIONS

CEC	cation exchange capacity
FF	face-to-face
EF	edge-to-face
EE	edge-to-edge
CME	clay modified electrode
CV	cyclic voltammetry
SCE	saturated calomel electrode
SEM	scanning electron microscopy
SPCME	spin-coating clay modified electrode

# CHAPTER I

## INTRODUCTION

### **I.Statement of the Problem**

The primary goal of this project is to study the swelling and shrinking behavior of orientated SWy-1 and SAz-1 clay films.

The swelling and shrinking properties of clay beds has an important impact on the transport of pollutants through the environment especially the leachate generated in waste disposal landfills. The transition of a clay bed from a swollen to a collapsed configuration clearly is important in affecting pollutant transport. The studies of swelling properties at clay beds can also be used in the agricultural and construction fields such as the soil fertility, roads, and houses. It can also lead to the studies of the fundamental physical chemistry as well as the electrochemistry applications. For example, the clay bed can be used to study the diffusion mechanism (including factors such as energy and forces involved) of species passing through it.

### **II.Clay Chemistry Background**

Clays are ubiquitous minerals, components of many soils and sediments. They have long been used as catalysts (1). Such materials are of interest for a number of reasons. They are often very stable and chemically robust materials; for

example; they can withstand high temperatures and highly oxidizing conditions. Perhaps the greatest interest in the clays, however, arises because they have known and well-defined structures. One of the biggest advantages of clays is that they are natural species which are very abundant and inexpensive. Clays are colloidal, layered hydrous aluminosilicates, most of which occur naturally and belong to the class of minerals called phyllosilicates (e.g., montmorillonites, kaolinites, hectorites, nontronites). The layers in these clays are assembled from sheets of  $\text{SiO}_4$  tetrahedra (Te) and  $\text{AlO}_6$  octahedra (Oc). In the widely used smectite, montmorillonite, each layer of the clay is composed of an Al-octahedral sheet sandwiched between two Si-tetrahedral sheets, with the oxygen atoms on the apices of the tetrahedra shared with the octahedra. Montmorillonites are referred to as 2:1 or Te-Oc-Te clays. The 1:1 or Te-Oc clays have layers which are composed of one tetrahedral and one octahedral sheet.

Of special interest are the swelling (or expanding) clays known as smectite clays (2,3,4). There are four unique properties of smectite clays: a) cation exchange, b) intercalation, c) swelling, and d) ability to expand beyond a single molecular layer of intercalant. The extent of interlayer swelling depends on the nature of the swelling agent, the exchange cation, the layer charge, and the location of the layer charge (5). The negative charge is obtained from the isomorphous substitution of  $\text{Si}^{4+}$  by  $\text{Al}^{3+}$  (or  $\text{Fe}^{3+}$ ) in tetrahedral positions or  $\text{Al}^{3+}$  by  $\text{Mg}^{2+}$  (or  $\text{Fe}^{3+}$ ). The layer charge in octahedrally charged smectites is distributed over all oxygens in the framework. This excess charge is compensated by exchangeable cations (e.g.,  $\text{Na}^+$ ,  $\text{Ca}^{2+}$ ) adsorbed on the surface of the layers. Since

the exchangeable cations compensate the unbalanced charge in the interior of the layers due to isomorphous substitution, the cation exchange capacity (CEC) is a measure of the degree of substitution. The charge distribution in tetrahedral layer and in octahedral layer, the CEC, and the formulae of SWy-1 and SAz-1 clay are listed in **Table 1** (6,7,8,9).

Most clay minerals consists of particles containing several layers stacked parallel to one another to form plates. The cohesive forces between the layers are primarily electrostatic and van der Waals forces. The main attractive force is the electrostatic interaction of the negatively charged layers and positively charged interlayer material, frequently an alkali or alkaline earth cation. The main repulsive forces arise from two ways as described as follows:

a) It arises from the solvation of interlayer cations (in natural systems, hydration) supplemented by that from interaction of the solvate (intercalate) with the surface oxygens of the 2:1 layers (6). The interlayer cations are often hydrated and readily exchangeable. The interlayer spacing (or basal spacing) depends mainly upon the extent of hydration of the exchangeable cations.

b) It arises from the electrostatic repulsion of two negatively charged plates.

On the other hand, the exposure of clay to electrolyte can also cause changes in the orientation of individual clay platelets with respect to each other.

The clay layer structures and swelling properties are elucidated as follows:

#### A) Swelling of the clay

First of all, the clay mineral montmorillonite has the ability to adsorb a large

**TABLE 1 SWy-1 and SAz-1 Clay Data**

	<u>Sample</u>	
	<u>SWy-1</u>	<u>SAz-1</u>
tetrahedral layer(esu/unit cell) <sup>a</sup>	0.16	0.14
octahedral layer(esu/unit cell) <sup>b</sup>	0.52	1.00
total charge(esu/unit cell) <sup>c</sup>	0.68	1.14
CEC (meq/100g) <sup>d</sup>	76.4	120
formula <sup>e,f</sup>	(Al <sub>2.94</sub> Fe <sup>3+</sup> <sub>0.32</sub> Fe <sup>2+</sup> <sub>0.03</sub> Mg <sub>0.58</sub> ) (Si <sub>8.0</sub> )O <sub>20</sub> (OH) <sub>4</sub>	(Al <sub>2.8</sub> Fe <sup>3+</sup> <sub>0.34</sub> Mg <sub>0.86</sub> ) (Si <sub>7.6</sub> Al <sub>0.24</sub> )O <sub>20</sub> (OH) <sub>4</sub>

<sup>a,b,c</sup> These data are cited from reference (7)

<sup>d</sup> These data are cited from reference (8)

<sup>e,f</sup> The SWy-1 formula is computed by Dr. Alanah Fitch at Department of chemistry, Loyola University of Chicago; The SAz-1 formula is cited from reference (9)



amount of water by i) hydration of intercalated cations and by ii) an interaction of interlayer water with the clay surface. Addition of exchangeable cations to suspended clay particles in distilled water will reduce the negative layer charges and allow clay plates to come together. Norrish and Quirk (10) showed that the concentration of an electrolyte in which montmorillonite was immersed could be used to control its swelling, the interlayer spacing increasing with decreasing electrolyte concentration. Thus, interlayer solvation (or hydration) exerts a repulsive force between the silicate layers and leads to expansion. On the other hand, if electrostatic attractive forces between the negatively-charged silicate layers and the positively-charged interlayer cations dominate, then the repulsive forces do not lead to expansion (7). It is generally agreed, however, that swelling, or lack of it, is controlled by the balance of attractive and repulsive forces between adjacent 2:1 layers.

#### B) Orientation of clay films

When the clay plates aggregate into larger particles, three modes of association occur: face-to-face (FF), edge-to-face (EF), and edge-to-edge (EE). The EF and EE associations lead to more voluminous "house-of-cards" structures (2,3,11). By spin coating the clay, FF structure is expected.

#### C) Charge of the clay

From the above SWy-1 and SAz-1 clay data, it is obvious that SAz-1 clay carries higher total charge (1.14 esu/unit cell) than SWy-1 clay (0.68 esu/unit cell). Although the amount of charge in the tetrahedral layer are close to equal (0.16

esu/unit cell for SWy-1 and 0.14 esu/unit cell for SAz-1), the amount of charge in the octahedral layer is different for these two clays (0.52 esu/unit cell for SWy-1 and 1.00 esu/unit cell for SAz-1). Their charge difference may be significant since Schultz (12) and Horvath and Novak (13) claim that the total charge is the controlling factor influencing expansion properties.

In order to explain how charge of the clay affects swelling in different electrolyte concentrations, it is necessary to briefly introduce the classical theory of electrical double layer. The electrical double layer is made up of two layers: the inner layer (or called Stern layer) and the diffuse layer. The inner layer is the layer closest to the charged surface. It contains solvent molecules and sometimes other species (ions or molecules) that are said to be specifically adsorbed. The diffuse layer is composed of nonspecifically adsorbed ions which extends from the Stern layer into the bulk of the solution. The thickness of the electrical double layer depends on the total ionic concentration in the solution (14). The computation of the ion distribution in the electrical double layer as a function of the electrolyte content of the bulk solution shows that the double layer is compressed toward the surface when the bulk electrolyte concentration is increased. This allows platelets to more closely approach each other before experiencing large repulsion force. Thus, the net result of the attractive (van der Waals force) (3) and the repulsive force depends upon the concentration of the electrolyte which also affects the swelling of the clay film.

From the above classical double layer theory description, we can see that it plays a significant part in determining the swelling of clays. In film studies, we find

that our results of SAz-1 (Ca form) clay can not exactly be accounted for by the double layer theory.

### **III.Goal of Clay Chemistry Study**

Our goal in this study is to study how swelling in clays is affected by charge of the clay and by electrolyte. We seek to determine if swelling is primarily driven by electrostatic effects (double layer repulsion) or by hydration effects. In the former case, the charge of the clay should play a significant role. In the latter case, charge of the clay should be relatively unimportant.

### **IV.Technique: Cyclic Voltammetry (CV)**

In this project, we study swelling properties of clays using electrochemical techniques. Our primary technique is cyclic voltammetry (CV). CV monitors the electrode current of an electroactive species as the electrode potential is changed. The potential starts from a value positive of the potential of an oxidized substrate, and is then scanned in the negative direction. As the potential approaches the formal potential, a Faradaic current is observed, which is due to the reduction of compound at the electrode surface when the electrode potential is negative of the half-wave potential ( $E_{1/2}$ ) by an amount  $59/2n$  mv ( $n$  is the number of electrons involved)(for a reversible couple), the current peaks out. As the scan is continued in the negative direction, the reduction current decreases due to a depletion of the substrate in the diffusion layer. At the instant the scan is reversed, the observed current is still due to the substrate reduction since the potential is negative of the

formal potential. Upon scanning positive, a Faradaic current of opposite sign appears as the substrate is regenerated through an oxidation reaction. There will be a corresponding oxidation peak at  $59/2n$  mv positive of  $E_{1/2}$ . The voltammogram is a display of current (vertical axis) vs. potential (horizontal axis). A typical cyclic voltammogram is shown in **Fig. 1**.

The peak current for a reversible system is described by the Randles-Sevcik expression (See section I in Chapter III for detail) (15,16,17).

$$i_p = 2.69 \times 10^5 n^{3/2} A D^{1/2} C^* \nu^{1/2} \quad [1]$$

where  $i_p$  = peak current, A

$n$  = number of electrons

$A$  = electrode area,  $\text{cm}^2$

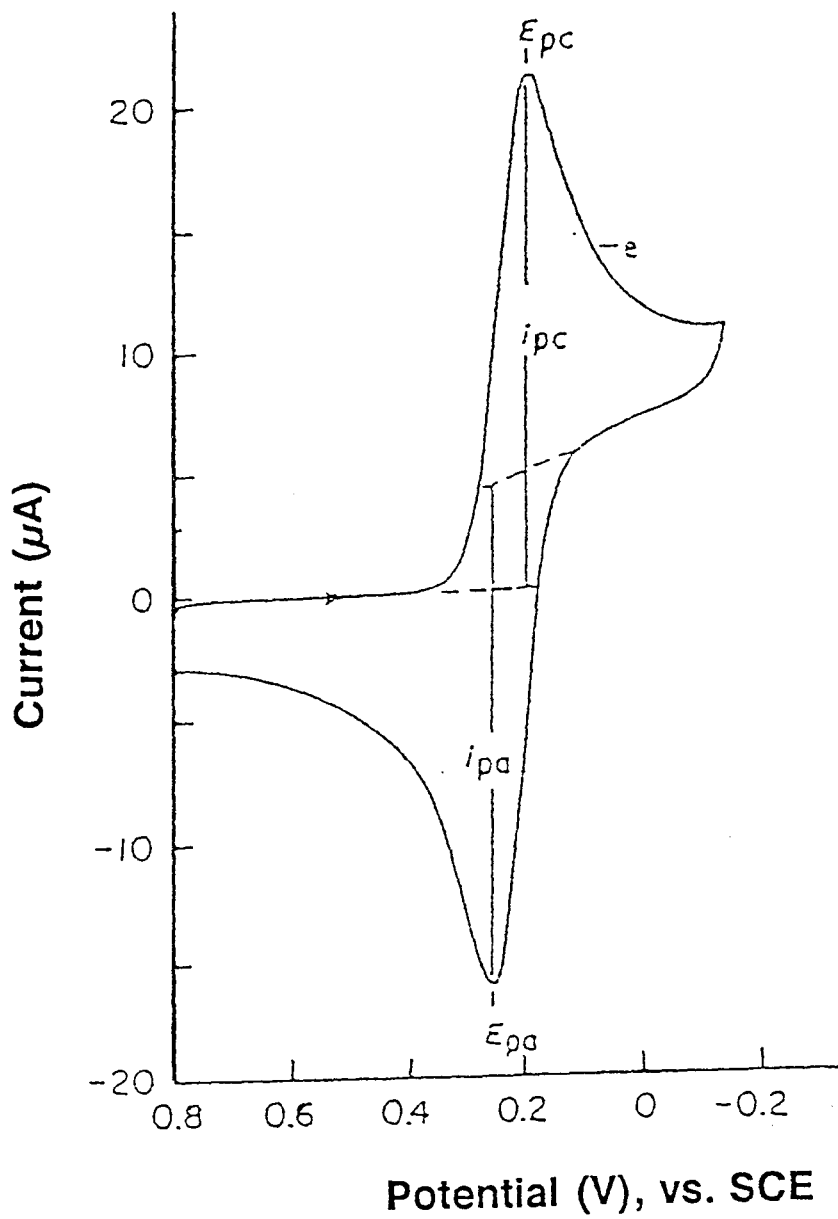
$D$  = diffusion coefficient,  $\text{cm}^2/\text{s}$

$C^*$  = concentration,  $\text{mol}/\text{cm}^3$

$\nu$  = scan rate,  $\text{V}/\text{S}$

It is important to note from equation [1] that the measured current depends on  $D^{1/2}$ , the diffusion coefficient for the substrate. Thus, by measuring current, we are measuring the diffusion of a substrate which can change with the medium. In this study we monitor how the current for an anionic probe  $[\text{Fe}(\text{CN})_6]^{3-}$  is affected by clay swelling. Clay swelling is being related to the current obtained from CV. When the clay swells, more probe molecules are able to arrive at the electrode surface. Thus, larger peak current is detected. The reason that anionic probe is

**Fig. 1 A display of typical cyclic voltammogram of 6 mM  $K_3[Fe(CN)_6]$  in 1.0 M  $KNO_3$ .**



used in this study is the probe should penetrate through the negatively charged clay films to the electrode surface without being trapped between the clay layers. Thus, it should not affect the peak current determination.

Preparation of clay membranes is feasible. The first such membranes were prepared as long ago as 1939 by soil scientist C.E.Marshall (18). In this project, we use the techniques of modified electrodes (19,20), specifically clay-modified electrode (CME). CME have since been prepared with a great deal of variation in stability and conductivities from lab to lab (19). A large number of CME studies have been conducted (21,22,23,24,25,26,27,28,29,30,31). Many of these studies centered on forming electronically conducting domains within the interlayer region.

In this study, we relate the ratio ( $I_{pcme}/I_{pbare}$ ) data to the interlayer spacing between two clay platelets. The methodology used here (CME) should be more useful than low angle X-ray diffraction (XRD) since XRD measurements are difficult to make and difficult to interpret. Norrish (32) first showed the effect of sodium on the interlayer spacing in the large swelling region via XRD measurements. Subsequent experiments have been difficult to reproduce (33,34,35,36,37,38) due to the effect of particle screening introducing diffraction pattern artifacts, and via spurious peaks. Also, a deconvolution function is required to abstract the true long distance diffraction patterns (18).

## **V.Synopsis of Experiments**

In the following chapters of experimental and results and discussion sections, many experiments have been performed starting from the

characterization of the Pt working electrode, the Scanning Electron Microscopy (SEM) study of the clay film integrity and thickness, the Spin Coated Clay-Modified Electrode (SPCME) study of the clay film stability as a function of time, and also the determination of the position of the diffusion layer. All the above mentioned preliminary experiments conducted are to establish a consistent condition for later electrolyte, charge, and probe effect studies. This is the most critical but important step in the whole project. Following this, the swelling studies of both SWy-1 and SAz-1 clay are done. We choose to study SAz-1 vs. SWy-1 clay for three reasons: 1) they carry different amount of total charge and octahedral layer charge (SAz-1 carries a higher charge than SWy-1 does), 2) SAz-1 is Ca-saturated form while SWy-1 is Na-saturated form, and 3) their CEC values are quite different. By comparing these two types of clay, we hope to further understand the effect of the charge in the swelling of clay films as well as the differences on electrolyte swelling effect between them.

In the SWy-1 clay study, the electrolyte (NaCl) concentration effect, (effect of added  $K^+$  effects ,that is,  $K_3[Fe(CN)_6]$  vs.  $Na_3[Fe(CN)_6]$ ), clay layer charge effect (oxidized vs. reduced SWy-1), and probe charge effect ( $Na_4[Fe(CN)_6]$  vs.  $Na_3[Fe(CN)_6]$ ) are elucidated. We predict that the  $Na_3[Fe(CN)_6]$  probe will create a more homogeneous environment inside the clay film than  $K_3[Fe(CN)_6]$  probe does. Thus, it is more precise to reflect the swelling of SWy-1 clay. For the probe charge effect, we expect the higher negative charge probe will be excluded more easily than the lower negative charge probe.

In the study of SAz-1 clay, two forms of SAz-1 (Ca and Na form) are studied.



For SAz-1 (Ca form), experiments of the effects of NaCl, KCl, and CaCl<sub>2</sub> concentration on the swelling of the clay film are conducted. On the other hand, NaCl and KCl concentration effects on SAz-1 (Na form) are compared with each other as well as with SWy-1 clay. We expect to see that SAz-1 (Na<sup>+</sup> form) has the similar swelling behavior as SWy-1 clay.

## **CHAPTER II**

### **EXPERIMENTAL METHODS**

#### **I. Experimental**

##### **I.1. General Methods**

###### **I.1.1. Instruments**

All cyclic voltammograms were obtained using an EG&G PAR 273 Potentiostat/Galvanostat with a Houston 2000 X-Y chart recorder or an EG&G VersaStat Potentiostat with an IBM HP 7371 plotter. Potentials were measured against a Saturated Calomel Electrode (SCE). Scanning Electron Microscopic (SEM) pictures were obtained on a StereoScan 240 Scanning Electron Microscope from Cambridge Instrument, Inc. Sample weighings were performed on a Sartorius Model 2443 analytical balance. Clay samples were centrifuged on Sorvall RC-5B Refrigerated SuperSpeed Centrifuge from Du Pont Instrument and then freeze-dried on Flexi-Dry lyophilizer from FTS Systems, Inc. Spin-coated clay samples for electrochemical studies were prepared on a MSR Analytical Rotor controlled by MSR Speed Control from Pine Instrument Company. Spin-coating clay samples for SEM were prepared on a vacuum spinner from Headway Research, Inc. Electrodes were polished on the Buehler ECOMET III Grinder/Polisher. Sonicating of the polished electrode was performed on Branson 1200 ultrasonic cleaner from Branson Ultrasonics Corporation.

### **I.1.2.Chemicals and Clay Samples**

Sodium chloride, potassium chloride, calcium chloride, and potassium ferricyanide were purchased from Aldrich. Sodium ferricyanide was from City Chemical Corporation. Sodium ferrocyanide was from Pfaltz & Bauer, Inc. Sodium ferricyanide was purified according to (31) prior to use. The rest of the chemicals were used as received.

## **II.Procedures**

### **II.1.1.Clay Sample Purification**

SWy-1 and SAz-1 clay were purified by suspension and sedimentation. They were made by the method of Jackson (39). A 10.00 g of clay was stirred in about 300 ml of deionized water for 48 hrs. Then the clay was centrifuged for 35 min at 20°C and 2400 rpm. The supernatant, which had a particle size less than 2  $\mu\text{m}$ , was collected. This suspension was then freeze dried in the lyophilizer overnight. The purified clay sample was stored in 20 ml scintillation vials wrapped with parafilm in a desiccator. A 0.105 g of purified clay sample was weighed and transferred to a 10 ml vial and 3 ml deionized water was added to obtain a 35 g/l concentration.

Na<sup>+</sup>-exchanged SAz-1 clay was prepared as follows: weigh 10.0 g of SAz-1 (Ca<sup>2+</sup> form), dissolved in 300 ml deionized water and then start stirring with a magnetic stir bar on the stirrer (VWR Model 320) for 48 hr. During that time the supernatant was occasionally decanted and new 2 M NaCl solution was added. The last supernatant was decanted and washed with deionized water. The decant

and wash process were repeated for at least 10 times. Each time the supernatant was checked by 0.1 M  $\text{AgNO}_3$  solution until no  $\text{AgCl}$  precipitation occurred. The clay suspension was then centrifuged as above. The rest of the procedures were the same as described above.

$\text{Na}^+$ -exchanged SWY-1 clay was prepared in the same way as  $\text{Na}^+$ -exchanged SAz-1 clay.

### **II.1.2.Preparation of the Analyte**

The analytes used were 4 mM  $\text{K}_3[\text{Fe}(\text{CN})_6]$ ,  $\text{Na}_3[\text{Fe}(\text{CN})_6]\cdot\text{H}_2\text{O}$  or  $\text{Na}_4[\text{Fe}(\text{CN})_6]$  unless otherwise specified. The received bulk  $\text{Na}_3[\text{Fe}(\text{CN})_6]\cdot\text{H}_2\text{O}$  must be purified prior to use. To 100 ml boiling deionized  $\text{H}_2\text{O}$  was added 50 g of  $\text{Na}_3[\text{Fe}(\text{CN})_6]\cdot\text{H}_2\text{O}$  in a 400 ml beaker equipped with a magnetic stir bar. The mixture was stirred until the sample was completely dissolved. It was allowed to cool to room temperature. The solution was then filtered by a filtering flask fitted with a glass filter frit and water suction. Dropwise 95% ethanol was added to the filtrate, swirling in the mean time, until a small amount of precipitate occurred. The beaker was wrapped with aluminum foil and kept overnight. It was filtered again. The precipitate collected was washed with a copious amount of 95% ethanol. The fine particle precipitate was placed on a piece of filter paper and covered with an aluminum-foil-wrapped funnel to avoid light and also left to air dry. At this point the purified  $\text{Na}_3[\text{Fe}(\text{CN})_6]$  was ready to use. Stock solutions were prepared as follows:

To a dry clean 25 ml volumetric flask was added 0.0329 g ( $1.0 \times 10^{-4}$  mol) of  $\text{K}_3[\text{Fe}(\text{CN})_6]$ , so that concentration would be 4 mM in 25 ml. The

desired concentration of electrolyte solution (such as NaCl, KCl etc.) was made up to the 25 ml mark, stoppered and shaken. For 4 mM  $\text{Na}_3[\text{Fe}(\text{CN})_6]$  and  $\text{Na}_4[\text{Fe}(\text{CN})_6]$ , 0.0299 g and 0.0484 g were added to the 25 ml volumetric flask. All the glassware used were cleaned with a laboratory detergent first, then rinsed with tap water and finally thoroughly rinsed with deionized water. The glassware was placed in a 100°C oven to dry and then allowed to cool to room temperature prior to use.

### **II.1.3.Preparation of Supporting Electrolyte**

Series concentrations of NaCl, KCl and  $\text{CaCl}_2$  solutions preparation were listed in **Table 2**, **Table 3**, and **Table 4**, respectively.

### **II.1.4.Electrochemical Experimental Setup**

The electrochemical system consists of three electrodes, two four-neck electrochemical cells, a potentiostat and either an X-Y chart recorder or an HP 7371 plotter. The EG&G PAR 273 PotentioStat was attached to a Houston 2000 X-Y charter recorder. The EG&G VersaStat PotentioStat was connected to an IBM HP 7371 plotter. The three electrodes were a Pt working electrode, Pt counter electrode, and a reference Saturated Calomel Electrode (SCE). One four-neck cell contained supporting electrolyte while the other contained analyte prepared by using electrolyte as solvent. Both cells were purged with  $\text{N}_2$  gas for 20 min before electrodes were submersed. Electrodes were always first placed into the electrolyte cell for taking a background scan, or so-called bare electrode scan,

**TABLE 2      NaCl Solution Preparation**

---

<u>NaCl Concentration (M)</u>	<u>Preparation</u>
2.0	116.8800 g of NaCl was weighed and transferred to a 1000 ml volumetric flask and was dissolved and diluted to mark with deionized H <sub>2</sub> O.
0.7	35 ml of 2 M NaCl was taken into a 100 ml volumetric flask and was diluted to mark with deionized H <sub>2</sub> O.
0.2	10 ml of 2 M NaCl was transferred into a 100 ml volumetric flask and was diluted to mark with deionized H <sub>2</sub> O.
0.05	25 ml of 2 M NaCl was transferred into a 1000 ml volumetric flask and was diluted to mark with deionized H <sub>2</sub> O.

(TABLE 2 to be continued)

TABLE 2-Continued

---

<u>NaCL Concentration (M)</u>	<u>Preparation</u>
0.03	1.7532 g of NaCl was weighed and transferred into a 1000 ml volumetric flask and was diluted to mark with deionized H <sub>2</sub> O.
0.02	1.1688 g of NaCl was weighed and transferred into a 1000 ml volumetric flask and was diluted to mark with deionized H <sub>2</sub> O.
0.01	50 ml of 0.02 M NaCl was transferred into a 100 ml volumetric flask and was diluted to mark with deionized H <sub>2</sub> O.

---

**TABLE 3      KCl Solution Preparation**

---

<u>KCl Concentration (M)</u>	<u>Preparation</u>
4.0	149.1200 g of KCl was weighed and transferred into a 500 ml volumetric flask and was diluted to mark with deionized H <sub>2</sub> O.
2.0	50 ml of 4 M KCl was transferred into a 100 ml volumetric flask and was diluted to mark with deionized H <sub>2</sub> O.
0.7	35 ml of 2 M KCl was transferred into a 100 ml volumetric flask and was diluted to mark with deionized H <sub>2</sub> O.
0.2	20 ml of 2 M KCl was transferred into a 100 ml volumetric flask and was diluted to mark with deionized H <sub>2</sub> O.
0.05	25 ml of 2 M KCl was transferred into a 1000 ml volumetric flask and was diluted to mark with deionized H <sub>2</sub> O.

(TABLE 3 to be continued)



(TABLE 3-Continued)

---

<u>KCl Concentration (M)</u>	<u>Preparation</u>
0.03	2.2368 g of KCl was weighed and transferred into a 1000 ml volumetric flask and was diluted to mark with deionized H <sub>2</sub> O.
0.02	1.4912 g of KCl was weighed and transferred into a 1000 ml volumetric flask and was diluted to mark with deionized H <sub>2</sub> O.
0.01	50 ml of 0.02 M KCl was transferred into a 100 ml volumetric flask and was diluted to mark with deionized H <sub>2</sub> O.

---

**TABLE 4      CaCl<sub>2</sub> Solution Preparation**

---

<u>CaCl<sub>2</sub> Concentration (M)</u>	<u>Preparation</u>
2.0	221.9800 g of CaCl <sub>2</sub> was weighed and transferred to a 1000 ml volumetric flask and was dissolved and diluted to mark with deionized H <sub>2</sub> O.
0.7	35 ml of 2 M CaCl <sub>2</sub> was taken into a 100 ml volumetric flask and was diluted to mark with deionized H <sub>2</sub> O.
0.2	10 ml of 2 M CaCl <sub>2</sub> was transferred into a 100 ml volumetric flask and was diluted to mark with deionized H <sub>2</sub> O.
0.05	25 ml of 2 M CaCl <sub>2</sub> was transferred into a 1000 ml volumetric flask and was diluted to mark with deionized H <sub>2</sub> O.

(TABLE 4 to be continued)

(TABLE 4-Continued)

---

<u>CaCl<sub>2</sub> Concentration (M)</u>	<u>Preparation</u>
0.03	3.3297 g of CaCl <sub>2</sub> was weighed and transferred into a 1000 ml volumetric flask and was diluted to mark with deionized H <sub>2</sub> O.
0.02	2.2198 g of CaCl <sub>2</sub> was weighed and transferred to a 1000 ml volumetric flask and was diluted to mark with deionized H <sub>2</sub> O.
0.01	50 ml of 0.02 M CaCl <sub>2</sub> was transferred into a 100 ml volumetric flask and was diluted to mark with deionized H <sub>2</sub> O.

---

before each run. At this point the  $N_2$  gas was blanketing over the surface of the solution. This was done by lifting the  $N_2$  gas tube from the solution and adjusting the flow rate of the gas stream to a degree that a slight vibration on the surface of the solution was reached. This was to avoid the oxygen interference and gas stream disturbance during the entire experiment period. Chart recorder was calibrated before use. X direction (V/inch) and Y direction ( $\mu A$ /inch) were set according to the specific needs. The electrodes were attached to the corresponding cables on the potentiostat. Potentiostat parameters were set prior to execution. For standard experiment, scan rate of 50 mv/s, low pass filters and potential windows of +0.8V to -0.2V were consistently used in this work unless specified. If the EG&G PAR 273 potentiostat was used, desirable current scale and high stability mode must be set prior to use.

### **II.1.5. Procedures of Cleaning the Pt Electrode**

Pt working electrodes must be polished and sonicated prior to use. This was to make the Pt surface as clean and fresh as possible. It was carried out with a slurry of  $0.2\mu$  alumina (Buehler Inc., Lake Bluff, IL) and copious amounts of deionized water on a felt buffing pad, followed by ultrasonic cleaning in a beaker with deionized water for 5 minutes. The surface of the electrode was then rinsed with deionized water and wiped out with a Kimwipe.

### **II.1.6. Spin-Coating Clay Modified Electrode (SPCME) Fabrication**

A Pt working electrode was placed, Pt surface up, in the rotor rubber holder

of the MSR spinner. Its position was adjusted to where the electrode spun smoothly. The clay suspension container was shaken thoroughly each time prior to use. Then, gently, a 1  $\mu\text{l}$  of desired clay sample was applied on the Pt area of the electrode by using 10  $\mu\text{l}$  gas tight syringe. Next, the spinner speed control unit was turned on and adjusted until the electrode spun smoothly. Spin rate was then adjusted to 800 rpm. It was spun for 15 min until dry film was formed. The electrode was now ready for use.

### **II.1.7. Cyclic Voltammetric Scans in Both Electrolyte Background and in the Analyte Solution**

The Clay-Modified Electrode (CME) was dipped into the blanketed electrolyte solution for 10 min. Care was taken not to touch the clay part of the electrode against the cell. This was to establish equilibrium between the clay film and the electrolyte. After 10 min a background scan was taken by turning on the potentiostat cell and running a CV. It should show a smooth flat cyclic voltammogram without any peak. The CME was then transferred gently from the electrolyte cell to the blanketed analyte cell. The scans were repeated until two consecutive scans were superimposed on top of one another.

### **III. Pt Working Electrode Characterization**

The purpose of this experiment was to determine the active surface area of the Pt working electrode as well as to check the integrity of the electrode. In this experiment, six scan rates were used. The 2 M NaCl was used as the electrolyte

along with 4 mM  $K_3[(Fe(CN)_6)]$  as analyte. The procedures were carried out as described in II. Three replicates were done to show the relative error between each run. Between each run, the Pt working electrode was polished and sonicated.  $N_2$  gas blanket was kept during the whole experiment period. The VersaStat potentiostat and the electrochemical system as described in Section II was still used here.

#### **IV. Studies on SWy-1 CLay**

##### **IV.1.1. Scanning Electron Microscopy (SEM)**

A 16 mm x 12 mm x 0.508 mm Pt plate (from D.F. GoldSmith and Metal Corp., Chicago, IL) was placed on the suction holder of the spinner (Headway Research, Inc.). A 1  $\mu$ l sample of 35 g/l SWy-1 clay suspension was pipetted to the center of the Pt plate from the 10  $\mu$ l syringe. The power of the spinner was switched on, the vacuum pump turned on and the spin rate adjusted to 800 rpm. The sample was spun for 15 min. After the spinning was completed, the Pt plate was cut in half along the center of the sample area. A half piece was mounted on a nail-like aluminum plate by double-sided tape. Silver coating was put around the four sides of the Pt plate. When dried, the plate was put into the Hummer VI Sputtering system to coat a very thin layer of Au and Pd. Next it was then inserted in to the SEM vacuum chamber, positioned, and the magnification changed until the desired picture was obtained.

#### **IV.1.2.SPCME Stability**

The Spin Coating Clay-Modified Electrode (SPCME) was monitored in 4mM  $K_3[Fe(CN)_6]$  to determine the effect of the clay stability. The electrode was soaked in  $N_2$ -purged electrolyte containing 4mM  $K_3[Fe(CN)_6]$  for periods of 0-30 min with continuous cycling between the limit of +0.8 and -0.2V vs. Ag/AgCl reference electrode. Two electrolyte concentrations, 0.7 M and 0.2 M NaCl, were used, respectively. The  $K_3[Fe(CN)_6]$  reduction current at 50 mV/s was monitored every 5 min. The EG&G PAR 273 potentiostat/galvanostat system with the scan parameters listed in section II.1.4. was used.

#### **IV.1.3.Effect of Scan Rate on the CME Diffusion Layer**

Thirteen scan rates, ranged from 1 to 300 mV/s, were chosen to select one scan rate in which the diffusion layer would reside within the clay film on the CME during the entire time period required to complete one cycle. The EG&G PAR 273 potentiostat and Houston 2000 X-Y chart recorder system was used as described in section II.1.4. SPCME was made by the procedures outlined in II.1.6. 1  $\mu$ l of 35 g/l SWy-1 clay suspension was used throughout this experiment. All the solutions were purged and blanketed prior to use as described in section II.1.4. The analyte probe used was 4 mM solution of  $K_3[Fe(CN)_6]$ . The preparation procedures were outlined in section II.1.2. The electrolyte used was 0.7 M NaCl prepared as described in **Table 2**. The glassware was cleaned as described in II.1.2.

#### **IV.1.4. Effect of NaCl Concentration on the Swelling of SWY-1 Clay**

The purpose of this experiment was to compare the clay swelling behavior with the X-ray diffraction results. Seven different NaCl concentrations (See Table 1) were used with 4 mM  $K_3[Fe(CN)_6]$  as the probe. The experiment was conducted on the EG&G PAR 273 potentiostat system as described in II.1.4. 1  $\mu$ l of 35 g/l SWy-1 clay suspension was spin coated on the Pt electrode (See II.1.6.). Cyclic voltammetric scans were taken after 30 min. soaking in  $K_3[Fe(CN)_6]$ . For each concentration, three replicates were done. Each time both reduction current of CME and bare electrode were recorded. Ratio data were calculated out by dividing the peak current obtained on the CME,  $I_{p_{cme}}$ , over the peak current obtained on the bare electrode,  $I_{p_{bare}}$ . Between the two scans (CME and bare) repolishing and cleaning of the electrode was needed. In the low NaCl concentrations range, oxygen concentration was more sensitive to the cyclic voltammetric peak. Water vacuum suction degas of the solution was used in addition to the  $N_2$  purge. The water suction was done by pouring the solution directly from a 25 ml volumetric flask to a 50 ml filtering flask covered with a rubber stopper. A rubber tubing was connected between the outlet of the water suction and the inlet of the filtering flask. Degassing was undergone for about 3 min. until most of the bubbles were sucked out. The solution was then poured to the electrochemical cell and kept under  $N_2$  purge and blanket. CV was then taken.

#### **IV.1.5. Comparison Between $Na_3[Fe(CN)_6]$ Probe and $K_3[Fe(CN)_6]$ Probe**

This was to determine the probes'  $Na^+$  and  $K^+$  effect on the variability of the



ratio data from run to run, and 4 mM  $\text{Na}_3[\text{Fe}(\text{CN})_6]$  was used. The preparation of  $\text{Na}_3[\text{Fe}(\text{CN})_6]$  solution was described in II.1.2. CV were obtained on EG&G VersaStat PotentioStat system (See II.1.4.). The rest of the experiment was the same as the experiment outlined in III.1.5.

#### **IV.1.6.Comparison Between $\text{Na}_4[\text{Fe}(\text{CN})_6]$ Probe and $\text{Na}_3[\text{Fe}(\text{CN})_6]$ Probe**

This was to compare the probes carrying the same cation but different negative charges and to see the probe's charge effect on the swelling of the clay. The experiment was set up in a manner similar to that described in III.1.6. by using EG&G VersaStat PotentioStat system as outlined in II.1.4. The only difference was that 4 mM  $\text{Na}_4[\text{Fe}(\text{CN})_6]$  was used as prepared in II.1.2.

#### **IV.1.7.Effect of NaCl Concentration on SWY-1(reduced form)**

Reduced form SWY-1 clay sample was provided by J.W. Stucki's laboratory from the Department of Agronomy, University of Illinois at Urban. It was made by reducing  $\text{Fe}^{3+}$  in the clay lattice to  $\text{Fe}^{2+}$  state using the  $\text{Na}_2\text{S}_2\text{O}_4$  method (39). The EG&G VersaStat PotentioStat system was used. All the experiments were performed as described in IV.1.4.

### **V.Studies on SAz-1 Clay**

#### **V.1.1.Effect of NaCl Concentration on the Swelling of SAz-1( $\text{Ca}^{2+}$ form)**

The experiment was carried out using 4 mM  $\text{K}_3[\text{Fe}(\text{CN})_6]$  as probe, and 1  $\mu\text{l}$  of 35 g/l SAz-1 SPCME was used throughout this experiment. The EG&G

VersaStat PotentioStat systems were used as II.1.4. Conditions, such as NaCl concentrations, CME soaking time, and degassing procedures, were all the same as in IV.1.4.

#### **V.1.2.Effect of KCl Concentration on the Swelling of SAz-1(Ca<sup>2+</sup> form)**

A series of different concentrations of KCl were prepared as outlined in **Table 2**. The CME soaking time was also 30 min. EG&G VersaStat PotentioStat systems were described Chapter III, II.1.4. The purpose of this study was to see if the SAz-1(Ca<sup>2+</sup> form) clay platelets had the same layer collapse behavior as SWy-1 under the presence of high concentration of KCL. All the set up and procedures were same as V.1.1. except KCl was used instead of NaCl.

#### **V.1.3.Effect of CaCl<sub>2</sub> Concentration on the Swelling of SAz-1(Ca<sup>2+</sup> form)**

A series of concentrations of CaCl<sub>2</sub> were prepared as described in **Table 4**. The EG&G VersaStat PotentioStat system were used. A cyclic voltammogram of CME in the analyte solution was obtained after 30 min soaking in the analyte. All the procedures were same as V.1.1. except using CaCl<sub>2</sub> supporting electrolyte rather than NaCl.

#### **V.1.4.Effect of NaCl Concentration on the Swelling of SAz-1(Na<sup>+</sup>-exchanged form)**

Na<sup>+</sup>-exchanged SAz-1 clay was prepared as described in II.1.2. Series of different NaCl concentrations were applied as outlined in V.1.1. These experiments

were performed under the same conditions as in V.1.1. except that the clay used here was SAz-1 Na<sup>+</sup>-exchanged form.

#### **V.1.5.Effect of KCL Concentration on the Swelling of SAz-1(Na<sup>+</sup>-exchanged form)**

Similar to V.1.2., various KCl concentration experiments were done on Na<sup>+</sup>-exchanged SAz-1 clay. These experiments were done as in V.1.2.

## CHAPTER III

### RESULTS AND DISCUSSION

#### **I. Pt Working Electrode Characterization**

In order to use electrochemical techniques to study diffusion process in the clay film, the working electrode must be well characterized prior to use. The results of Pt working electrode characterization were shown in **Table 5** and **Fig.2**, respectively. The peak current in CV can be described by Randles-Sevcik equation (See section IV in Chapter I). Since  $n$ ,  $A$ ,  $D$  and  $C^*$  in the equation were all constant, a linear relationship between  $i_p$  and  $v^{1/2}$  was expected. From the regression data,  $R^2$  of 0.9997, x coefficient of 12.4235 and y-axis intercept of 0.3147 were obtained. By calculating through the equation, the active electrode area of  $0.471 \text{ mm}^2$  of diameter of 0.7746 mm was obtained. The average potential difference ( $E_{pc} - E_{pa}$ ) between the cathodic and anodic peak was from 65.5 mv to 75.7 mv for six scan rates. This was reasonably good, although the standard should be about 59 mv (15).

#### **II. Studies on SWy-1 Clay**

##### **1. Scanning Electron Microscopy (SEM)**

In order to use CME, it is important to verify that the film is intact and that all probe molecules arrive at the underlying electrode only by passing through

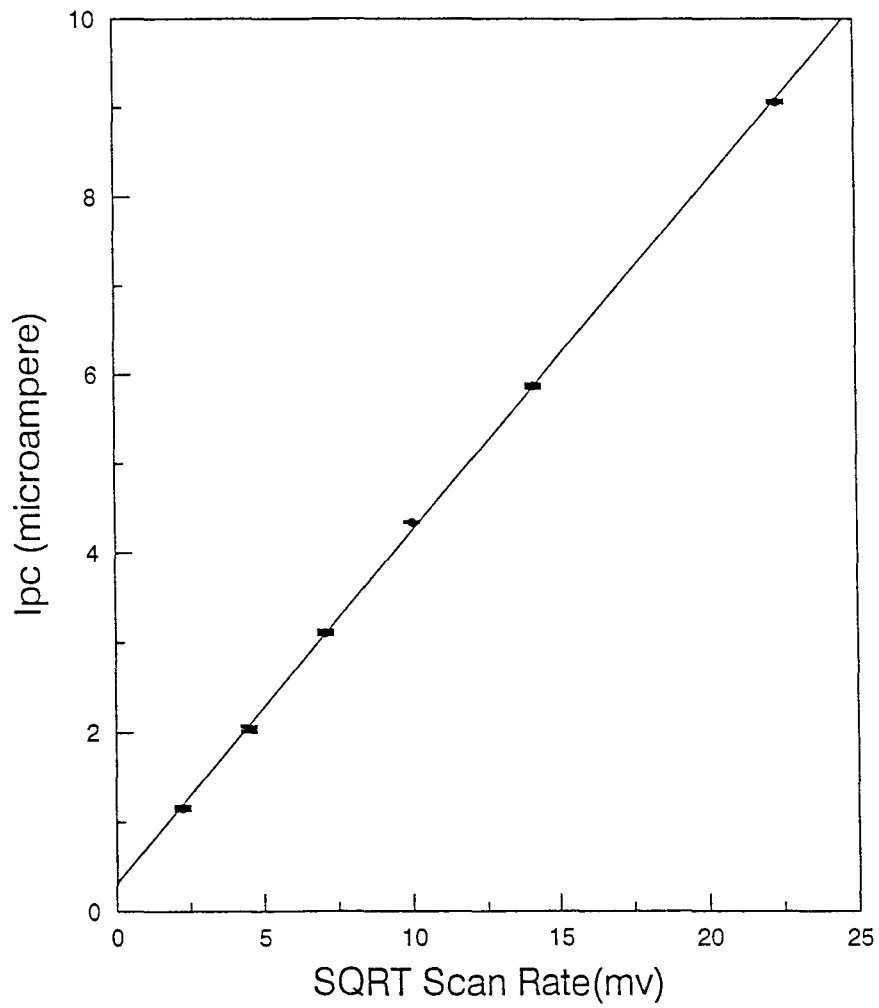
**TABLE 5 Pt Working Electrode Characterization Experiment Results**

---

<u>Scan Rate (v.V/S)</u>	<u>Average Peak Current (A)x10<sup>-6</sup></u>	<u>Average (Epc-Epa)(mv)</u>
5	1.5555	75.7
20	2.037	68.5
50	3.1043	66.2
100	4.3404	67.1
200	5.8698	65.6

---

**Fig. 2 A plot of the cathodic current vs. square root of scan rate for 4 mM  $K_3[Fe(CN)_6]$ , 2 M NaCl.**



the clay membrane. Thus SEM technique is used to meet this need. Fig. 3 is an SEM image we get from the top view of the clay surface. Since anions ordinarily are repelled by negatively charged clay layers, it has been suggested that the electroactivity arises from the presence of microchannels which are filled by solution containing the redox active anion. The grain boundaries in **Fig. 3** may represent the channels where redox active ions in solution can invade the film. This agrees with the results of SEM from King et al. (41). **Fig. 4** shows the picture of clay viewing from the back side which is in direct contact with the electrode surface. This encouraging result solved the unanswered question in our mind, that is, our spin-coated clay is not only being fully covered on the electrode surface but is homogeneously arranged by itself as well. No broken channels of clay bed are observed.

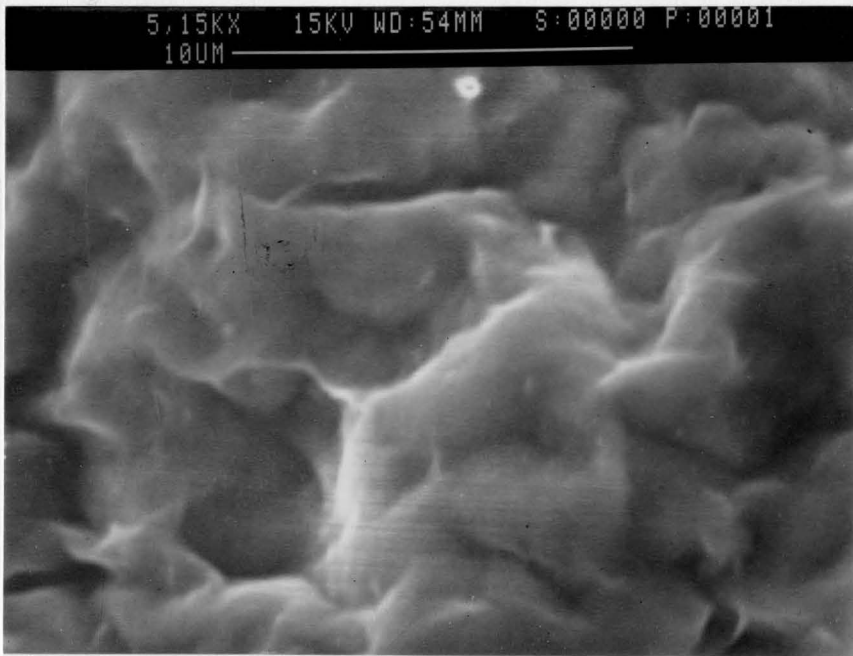
## **2.SPCME Stability**

SPCME stability test was done in order to prove that the clay was stable during the soaking period. Data for a 35  $\mu\text{g}$  CME soaking in  $\text{K}_3[\text{Fe}(\text{CN})_6]$  are shown in **Table 6** and **Fig. 5**, for 0.7 M and 0.2 M NaCl. Similar data were obtained for soaking in electrolyte followed by transfer to the  $\text{K}_3[\text{Fe}(\text{CN})_6]$  solution. For all quantities of clay, the currents were remarkably stable over the entire period (42). It showed that the clay was relatively more stable in high NaCl concentration solution than in low NaCl concentration solution. This agreed with Lee's (43) oven-dried CME results. Part of the reason that low NaCl concentration was less stable was that low concentration of NaCl may be related to high solution resistance (i.e



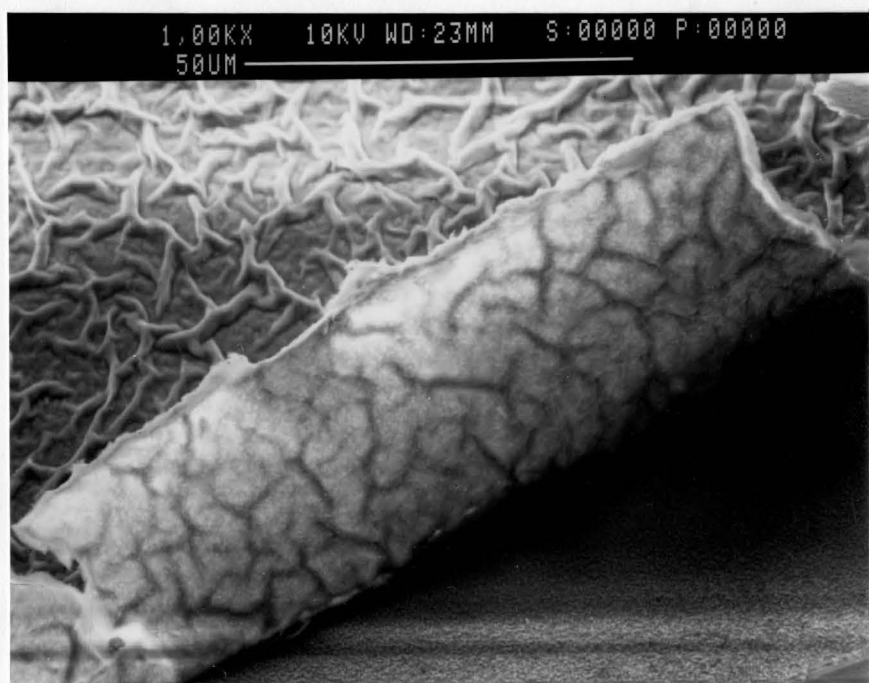
**Fig. 3. SEM image of 1  $\mu$ l SWy-1 spin-coated film from top topography.**

Fig. 4. SEM image of 1  $\mu$ l SWxy-Triplic-coated film; viewing from the back side



**Fig. 4. SEM image of 1  $\mu$ l SWy-1 spin-coated film viewing from the back side of the film.**

Fig. 5. A plot of the ratio of  $I_{an}$  over  $I_{cat}$  vs. soaking time for 4 mM  $Fe(CN)_6^{3-}$



**Fig. 5. A plot of the ratio of  $i_{pc}$  over  $i_{bare}$  vs. soaking time for 4 mM  $Fe(CN)_6^{3-}$  in 0.2 M and 0.7 M NaCl solutions.**

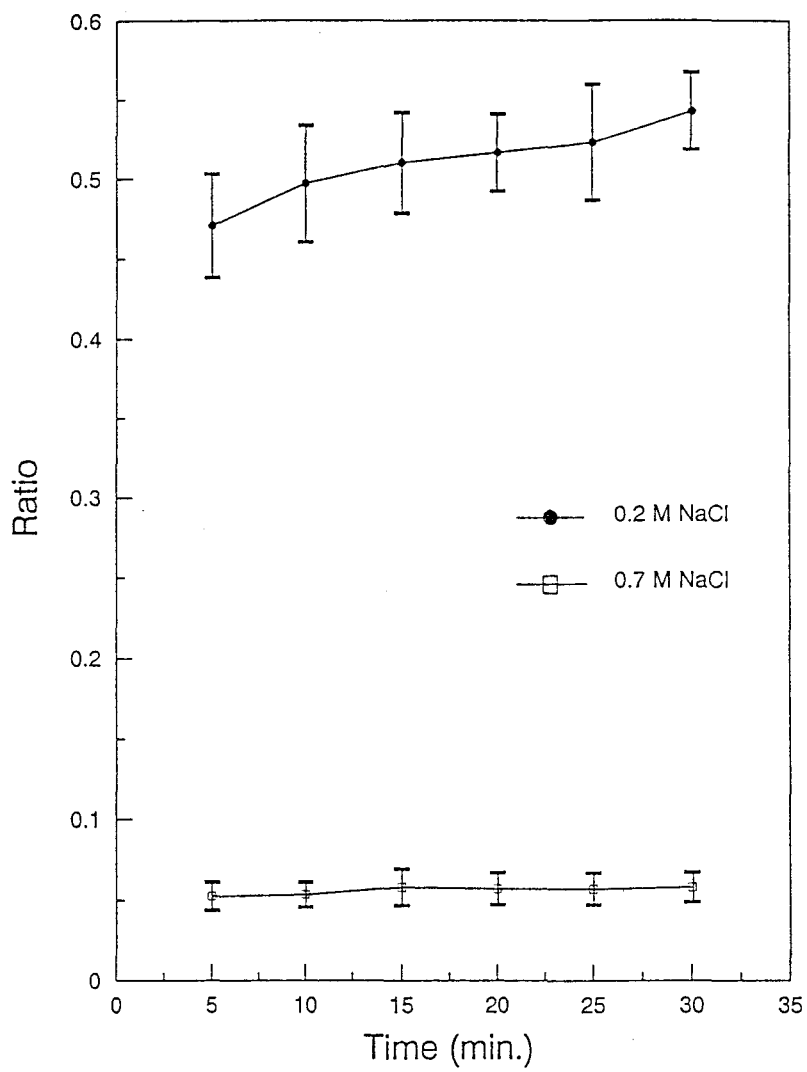


**TABLE 6 SPCME Stability Experiment Results**

---

<u>Time (min.)</u>	<u>Ratio (0.2 M NaCl)</u>	<u>Ratio (0.7 M NaCl)</u>
5	0.471 ± 0.032	0.052 ± 0.009
10	0.497 ± 0.037	0.053 ± 0.008
15	0.510 ± 0.032	0.058 ± 0.011
20	0.516 ± 0.024	0.057 ± 0.01
25	0.523 ± 0.037	0.057 ± 0.01
30	0.543 ± 0.024	0.058 ± 0.009

---

solution IR drop). In contrast, high concentration of NaCl corresponds to low solution resistance. When NaCl concentration decreased from 0.7 M to 0.2 M, the IR drop increased which may cause more error in determining the peak current.

### **3. Effect of Scan Rate on the CME Diffusion Layer**

In order to interpret the currents observed for our probe molecule, it was important to determine whether the currents arose from diffusion within the clay film or external to the clay film. A plot of the maximum reduction current (peak or plateau),  $I_{\max}$  vs.  $v^{1/2}$ , the scan rate to the half, showed the transition in cyclic voltammograms as a function of scan rate (**Fig. 6**). Tokuda's microhole array theory (44) predicts that a plot of  $I_{\max}$  vs.  $v^{1/2}$  should consist of two straight line portions. At low  $v^{1/2}$  values, when the diffusion layer ( $\delta$ ) is beyond the film thickness ( $L$ ) ( $\delta > L$ ), the current should be independent of scan rate (plateau-shaped cyclic voltammograms). At high  $v^{1/2}$  values, the diffusion layer ( $\delta$ ) does not have time to grow beyond the film ( $L$ ) ( $\delta < L$ ) and the current should vary linearly with  $v^{1/2}$  (peak-shaped cyclic voltammograms). These peak-shaped CVs contain information about the diffusion of the probe molecule within the clay film. This model was confirmed for 4 mM  $K_3[Fe(CN)_6]$  at 25, 30, 35  $\mu\text{g}$  film in 0.7 M NaCl (**Fig. 6**) as well as for 10, 15, 20 and 25  $\mu\text{g}$  films in 0.7 M NaCl and for the 35  $\mu\text{g}$  SAz-1 (Ca form) clay in 2 M NaCl (**Fig. 7**). One also expects that the slope of the  $v^{1/2}$ -dependent region of the plot should be the same for all film thicknesses, since it corresponds to diffusion occurs within the film regardless of total film length. The data shown



**Fig. 6 Maximum current obtained as a function of the scan rate for SWy-1 spin-coated Pt electrodes. The two straight line portions indicate that the electrode functions well as a microhole array. The numbers indicate the total mass ( $\mu\text{g}$ ) of clay applied.**

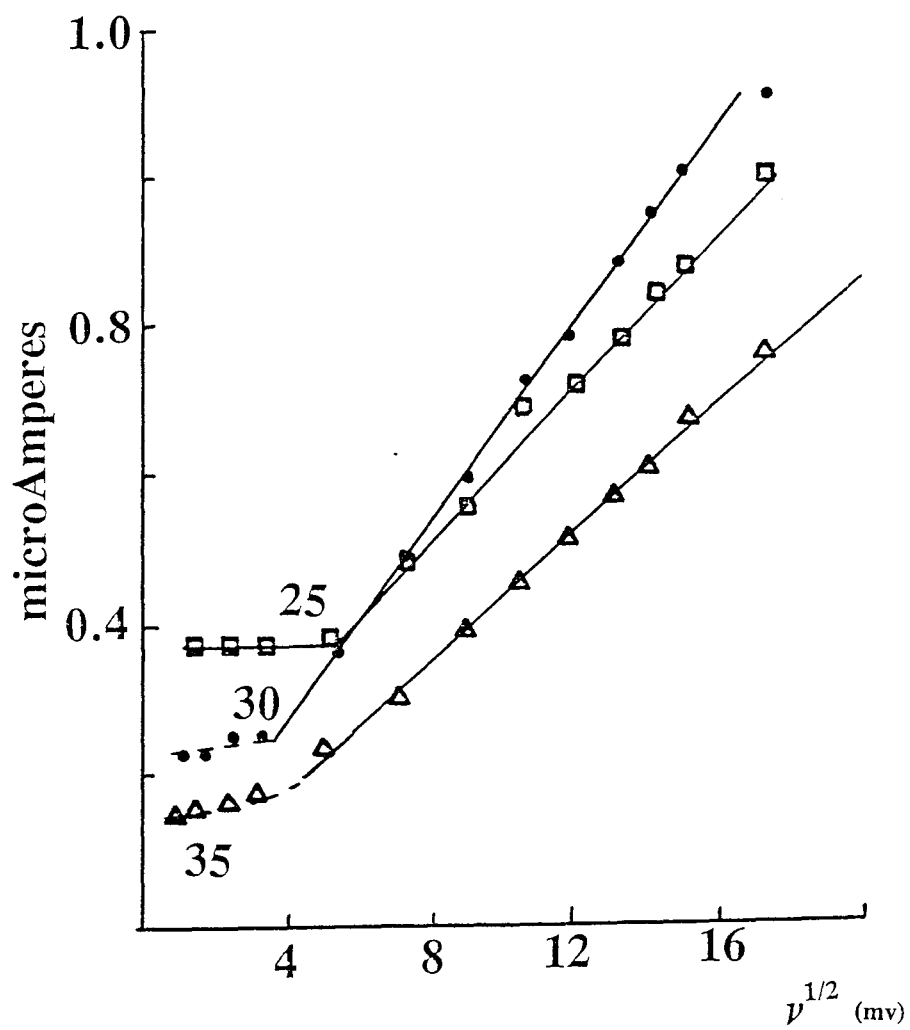
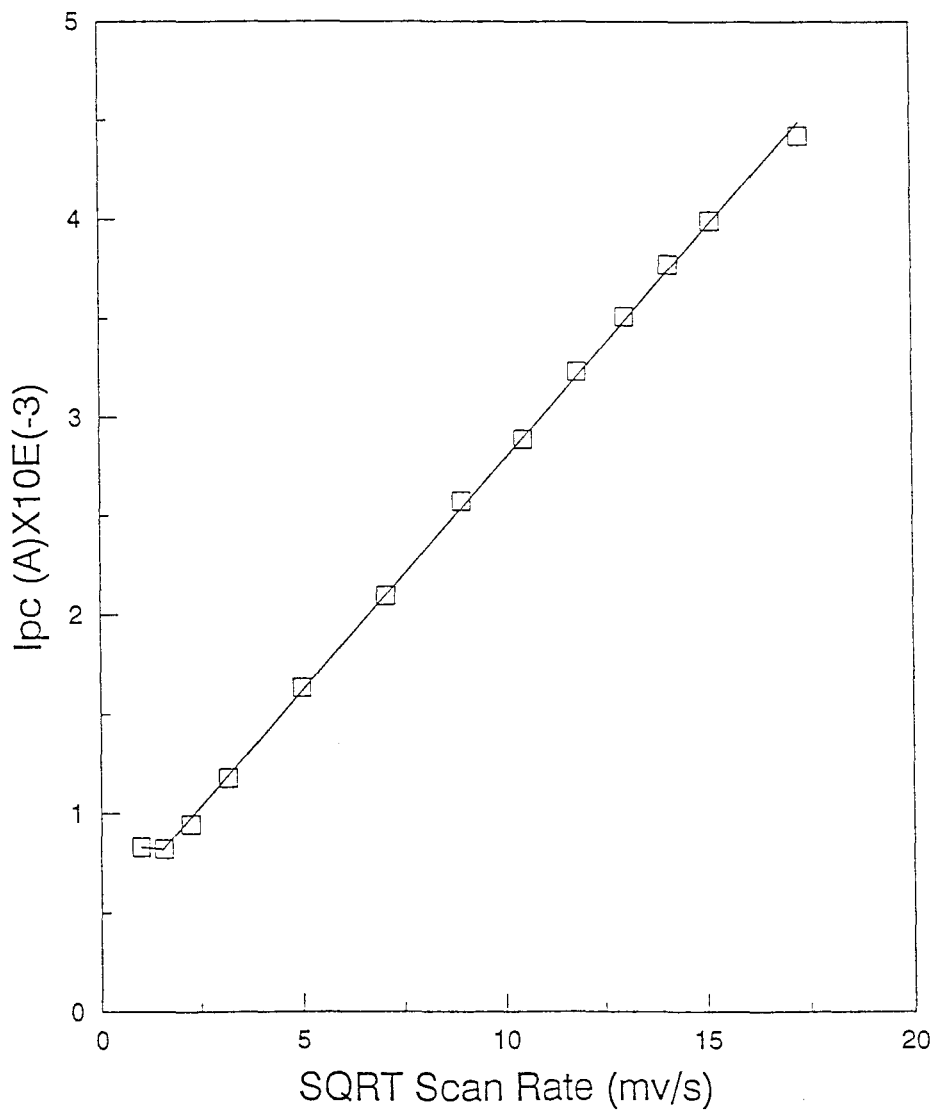


**Fig. 7 Maximum current obtained as a function of the scan rate for SAz-1 spin-coated Pt electrodes in 2 M NaCl.**



in **Fig. 6** show that the slope different for each film, indicating the variability in formation of fresh clay coatings (See also **Fig. 5** and **6**).

In the scan rate independence region, according to Tokuda's theory (44), the current depends on the clay film thickness. The following equation shows the relationship:

$$i_{ss} = nFADC^0/L \quad [2]$$

where

$i_{ss}$  = steady state current, A

$n$  = number of electrons

$F$  = the faraday constant, C

$A$  = electrode area,  $\text{cm}^2$

$D$  = diffusion coefficient,  $\text{cm}^2/\text{s}$

$C^0$  = bulk solution concentration,  $\text{mol}/\text{cm}^3$

$L$  = thickness of the film, cm

We can see that the steady state current ( $i_{ss}$ ) is inversely proportional to the film thickness ( $L$ ) since the rest of the parameters in equation [2] are constant in this case. Data in **Fig. 6** show that  $i_{ss}$  does, indeed, decrease with increasing amount of clay added to the film. We just indicated that from **Fig. 6** that we could distinguish between diffusion within vs. external to the film based on the  $v^{1/2}$  dependence of the current. Similar experiments were performed for CME in different electrolyte in order to determine an optimum scan rate when  $\delta < L$  for all electrolyte concentrations. In order to investigate the role of the double layer in long-distance swelling of clays, we proposed (45) that for a constant amount of clay applied to the electrode, and for a constant scan rate, changes in the

observed maximum reduction current as a function of electrolyte would reflect changes in the porosity of the film. This is true only if the diffusion layer resides within the film at that scan rate, over all electrolyte concentrations.

In **Fig. 8**, for 35  $\mu\text{g}$  clay electrodes,  $I_{\text{max}}$  is plotted as a function of the square root of the scan rate for the most compressed film (2 M NaCl) and the most expanded film (0.02 M NaCl). **Table 7** lists the data shown in **Fig. 8**. We see that a scan rate of 50 mv/s easily results in semi-infinite linear diffusion within the clay film for 2 M NaCl (arrow, **Fig. 8** inset). For 0.02 M NaCl, no break between  $v^{1/2}$ -dependent and  $v^{1/2}$ -independent behavior is observed. However, there are two distinct linear portions of the plot, each with a correlation coefficient greater than 0.99. We attribute this behavior to a transition from diffusion within the film ( $v^{1/2} > 7 \text{ (mv/s)}^{1/2}$ ) to diffusion external to the film ( $v^{1/2} < 7 \text{ (mv/s)}^{1/2}$ ). The lack of a distinct break could arise from the large size of the micropores present in the swollen film, which inhibits development of the microelectrode effect. The size of the micropores is established from the interlayer distance between platelets (42).

When the diffusion layer extends beyond the film, the current magnitude is governed by the value of the solution diffusion coefficient, just as in a bare electrode measurement. In order to confirm that the two slopes seen for 0.02M in **Fig. 8** can be attributed to diffusion within the clay film vs. diffusion extended to the film, we computed the ratio of two slopes. It should match the ratio of current obtained at a CME electrode to a bare electrode.

The ratio computed from the slopes (0.64) agreed well with that determined from the actual measurement of average ratio at 50 mv/s (0.7)(see also **Fig. 9**).

**Fig. 8 Scan rate dependence of the maximum cathodic current for 4 mM  $K_3[Fe(CN)_6]$  in 2 M (lower plot) and 0.02 M (upper plot) NaCl at 25  $\mu$ g spin-coated SWy-1 modified electrode. The arrow indicates that for both 0.02 M and 2 M NaCl the diffusion layer at 50 mv/s is semi-infinite in character and resides within the clay film. Inset: expanded graph for 2 M NaCl.**

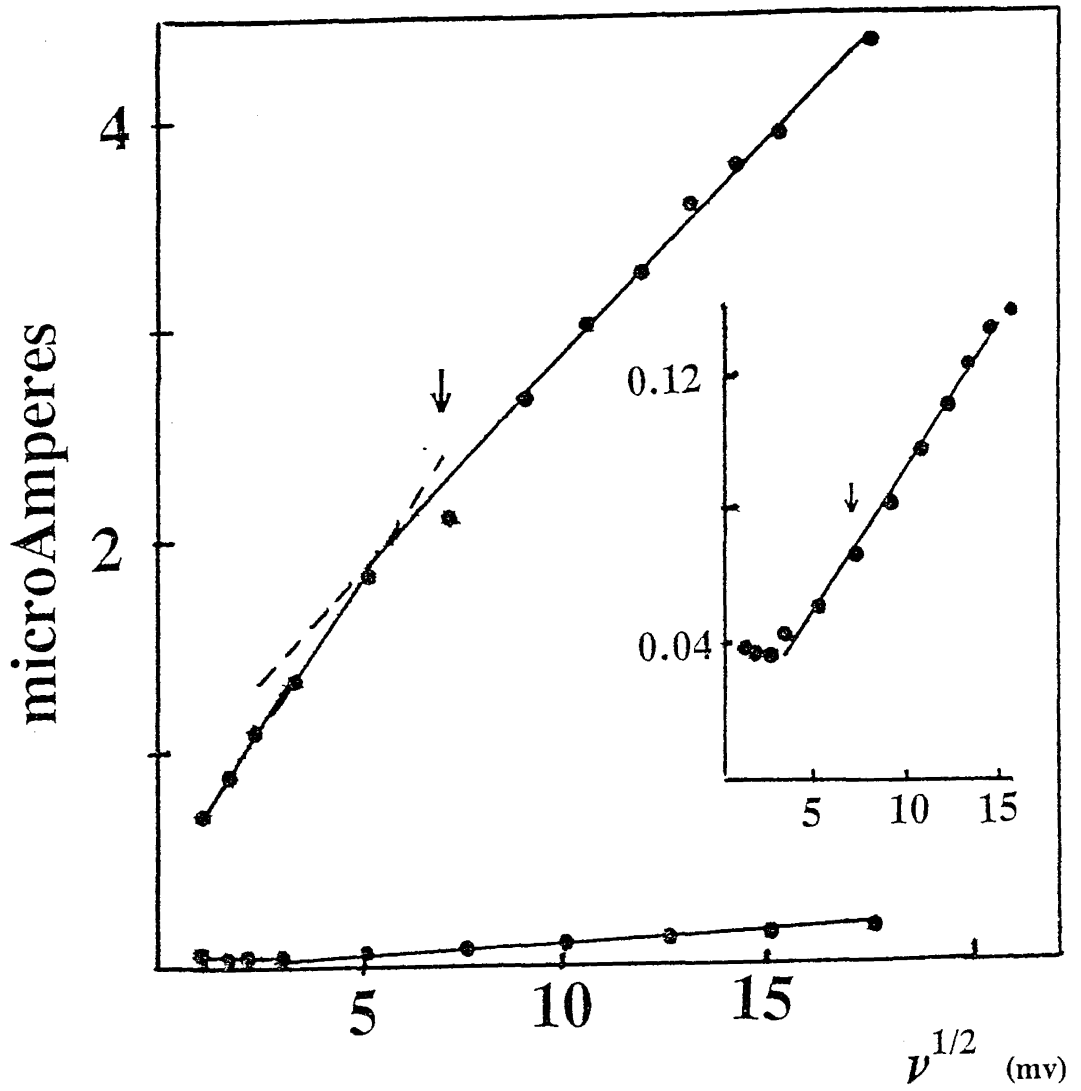




**Fig. 9 A plot of the ratio of  $i_{pc}$  over  $i_{bare}$  vs.  $1/\text{SQRT}[\text{NaCl}]$  for 4 mM  $[\text{Fe}(\text{CN})_6]^{3-}$  for 1  $\mu\text{l}$  of 35 g/l SWy-1 SPCME.**

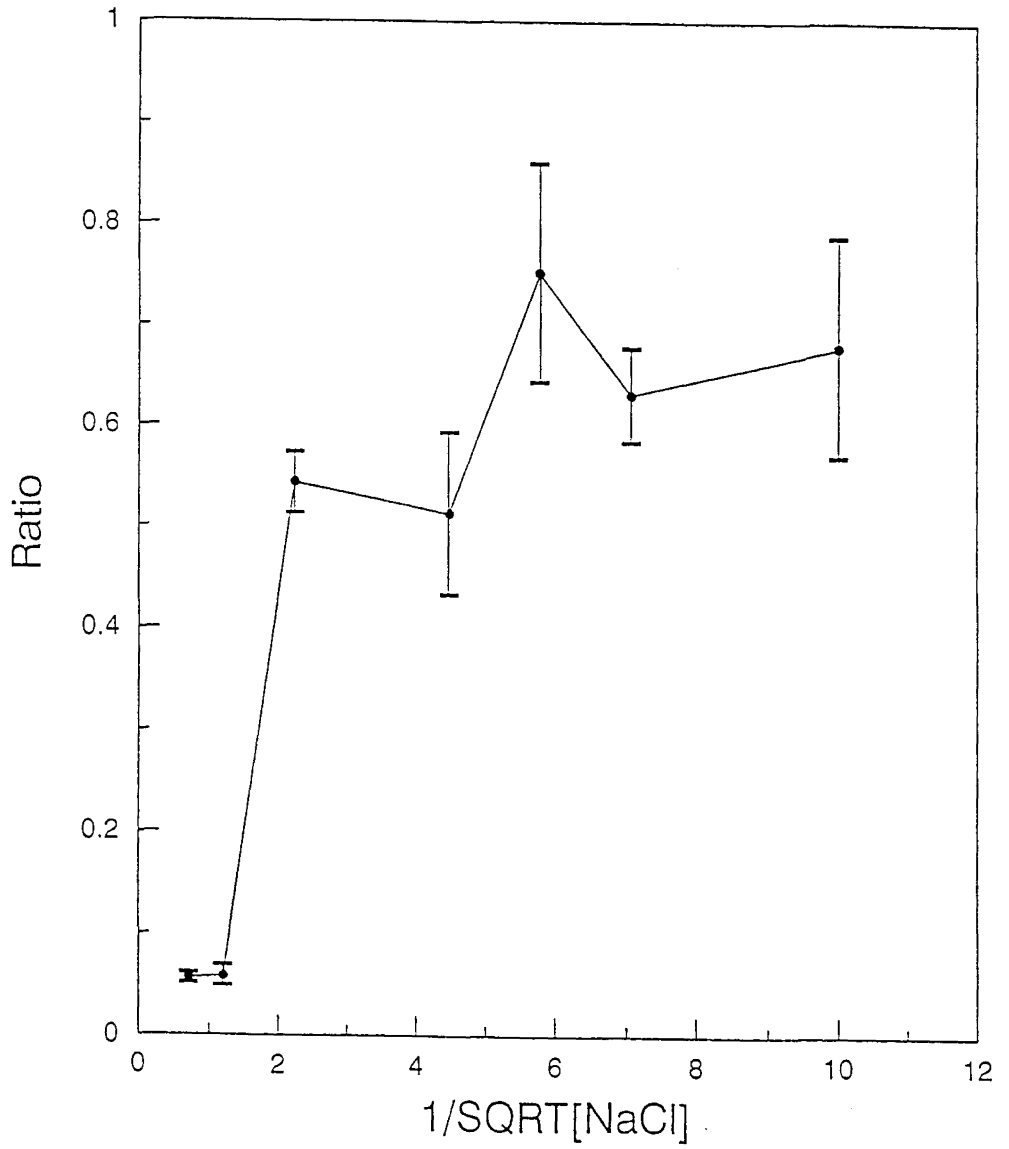


**TABLE 7 Scan Rate Dependence of the Maximum Cathodic Current for 4 mM  $K_3[Fe(CN)_6]$  in 2 M and 0.02 M NaCl at 25  $\mu$ g SWy-1 SPCME**

---

<u>Scan Rate(<math>v^{1/2}</math>) (mv/s)<sup>1/2</sup></u>	<u><math>I_p</math> (<math>\mu</math>A) (for 2 M NaCl)</u>	<u><math>I_p</math> (<math>\mu</math>A) (for 0.02 M NaCl)</u>
1	0.033	0.21
1.581	0.031	0.265
2.236	0.031	0.327
3.162	0.036	0.397
5	0.043	0.545
7.071	0.057	0.631
8.944	0.07	0.794
10.488	0.084	0.903
11.832	0.095	0.973
13.038	0.106	1.075
14.142	0.115	1.129
15.166	0.119	1.176
17.321	0.135	1.308

---

The agreement between these two values confirms our assignment of the origin of change in the slope of  $I_p$  vs.  $v^{1/2}$ . From the break in the slopes we can determine that a scan rate of 50 mv/s causes the diffusion layer to reside just within the film (arrow, **Fig. 8**)(42). According to this result, scan rate of 50 mv/s will be used consistently throughout the rest of experiments. This is to qualitatively require the diffusion layer to reside within the film by choosing the scan rate which is greater than the intercept transition scan rate.

#### **4.Effect of NaCl Concentration on the Swelling of SWy-1 Clay**

Based on these results, ratio values were determined for a 35  $\mu\text{g}$  film at 50 mv/s and plotted as a function of electrolyte dilution (**Fig. 9** and **Table 8**). These ratio data differ from those previously recorded (43), in that a 5-min measurement period was used previously, and a 5  $\mu\text{g}$  film was used. In the present results, it is interesting to speculate that a linear expansion of the film with electrolyte dilution is not observed (32,45); rather some step-wise expansion in the low electrolyte region may be observed (42). This may be attributed to the variability of the measurement due to the existence of the added  $\text{K}^+$  from the probe in the low electrolyte concentration region and/or the swelling process does behave step-wise hydration. The use of  $\text{Na}_3[\text{Fe}(\text{CN})_6]$  probe in the following experiment proves that the swelling of SWy-1 clay film is a step-wise process.

**TABLE 8 NaCl Effect on SWy-1 Clay**

---

<u>1/SQRT[NaCl] (M<sup>-1/2</sup>)</u>	<u>Ratio</u>
0.707	0.056 ± 0.005
1.195	0.058 ± 0.011
2.236	0.543 ± 0.03
4.472	0.513 ± 0.08
5.774	0.751 ± 0.171
7.071	0.631 ± 0.047
10	0.651 ± 0.175

---

## 5.Comparison among $\text{Na}_3[\text{Fe}(\text{CN})_6]$ , $\text{Na}_4[\text{Fe}(\text{CN})_6]$ Probe and $\text{K}_3[\text{Fe}(\text{CN})_6]$ Probe

The probe we used in the above experiment was  $\text{K}^+$  as cation. The magnitude of the error bars in **Fig. 9** was relatively large. We attributed this to the possible two factors: 1) cation competition between  $\text{K}^+$  and  $\text{Na}^+$  or 2) the large solution IR drop in the low electrolyte concentration region. In order to remove  $\text{K}^+$ ,  $\text{Na}_3[\text{Fe}(\text{CN})_6]$  and  $\text{Na}_4[\text{Fe}(\text{CN})_6]$  probes were used instead. **Fig. 10** and **Fig. 11** showed the results from  $\text{Na}_3[\text{Fe}(\text{CN})_6]$  and  $\text{Na}_4[\text{Fe}(\text{CN})_6]$  probes, respectively. Data were shown in **Table 9**. Smaller error bars were obtained than in **Fig. 9** for both  $\text{Na}^+$  probes, indicating that the presence of the second cation  $\text{K}^+$  promotes heterogeneity from sample to sample. This could be the result of multiple layering effects in which some interlayers contain  $\text{Na}^+$  and some  $\text{K}^+$ , which could vary from run to run. In another words, this caused the co-existence of the two different cation hydration states in the same clay film.

The ratio obtained for  $\text{Na}_3[\text{Fe}(\text{CN})_6]$  was higher (0.6) than the ratio obtained for  $\text{Na}_4[\text{Fe}(\text{CN})_6]$  (0.5)(compare **Fig. 10** and **11**), when the clay film was swollen (i.e in the low electrolyte concentration region). This data would be consistent with greater exclusion of the more negatively charged probe because of the repulsion between the negatively charged probe and the negatively charged clay platelets. The greater exclusion of the more negatively charge probe was in line with the electrical double layer theory as stated in section II in Chapter I which would result in exclusion of the anion probe from the film.

**Fig. 10 A plot of ratio ( $i_{pcme}/i_{bare}$ ) vs.  $1/\text{SQRT}[\text{NaCl}]$  obtained for 4 mM  $\text{Na}_3[\text{Fe}(\text{CN})_6]$  probe at 1  $\mu\text{l}$  35 g/l SWy-1 SPCME.**

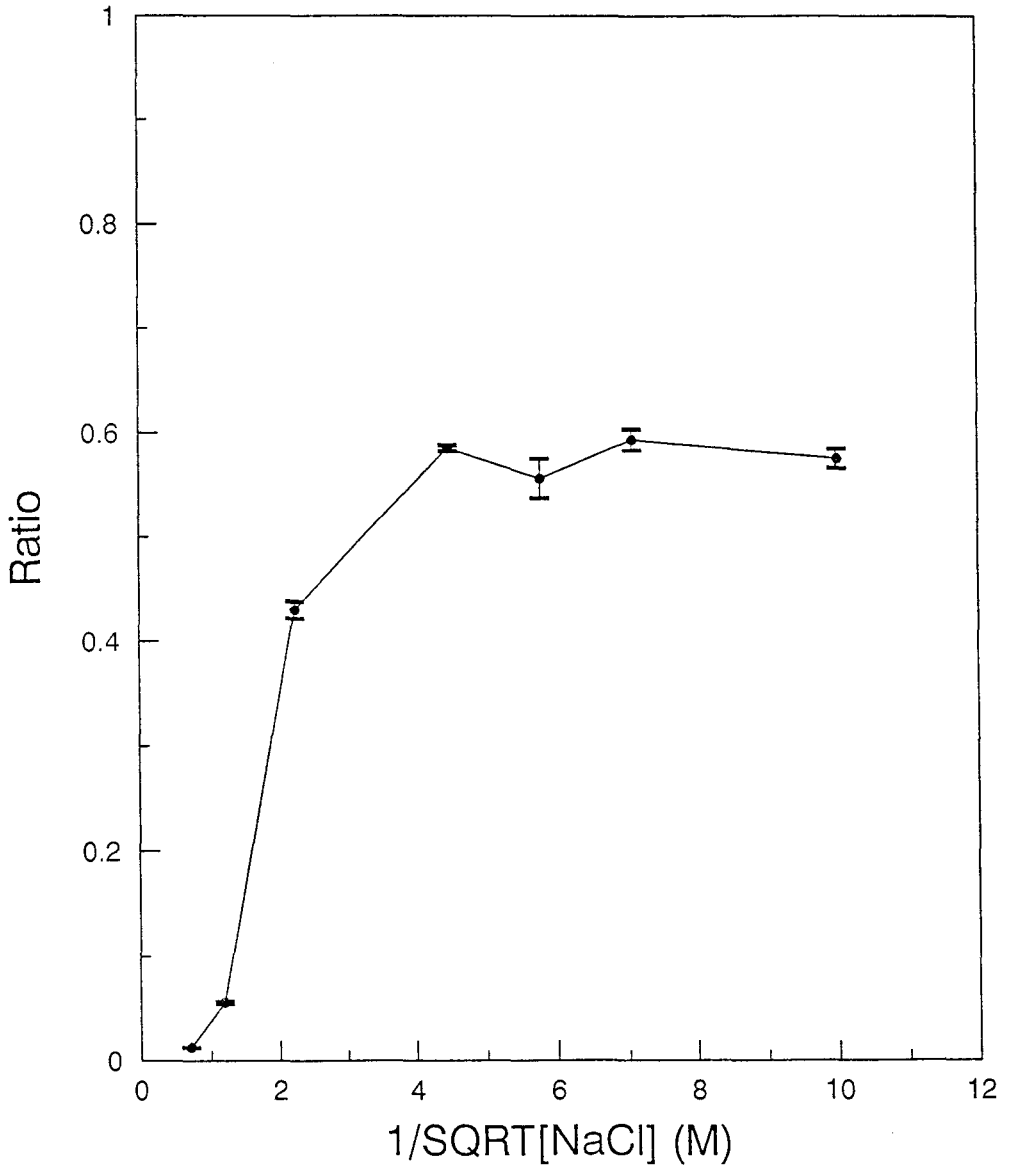




**Fig. 11 A plot of ratio ( $i_{pcme}/i_{bare}$ ) vs.  $1/\text{SQRT}[\text{NaCl}]$  obtained for 4 mM  $\text{Na}_4[\text{Fe}(\text{CN})_6]$  probe at 1  $\mu\text{l}$  35 g/l SWy-1 SPCME.**

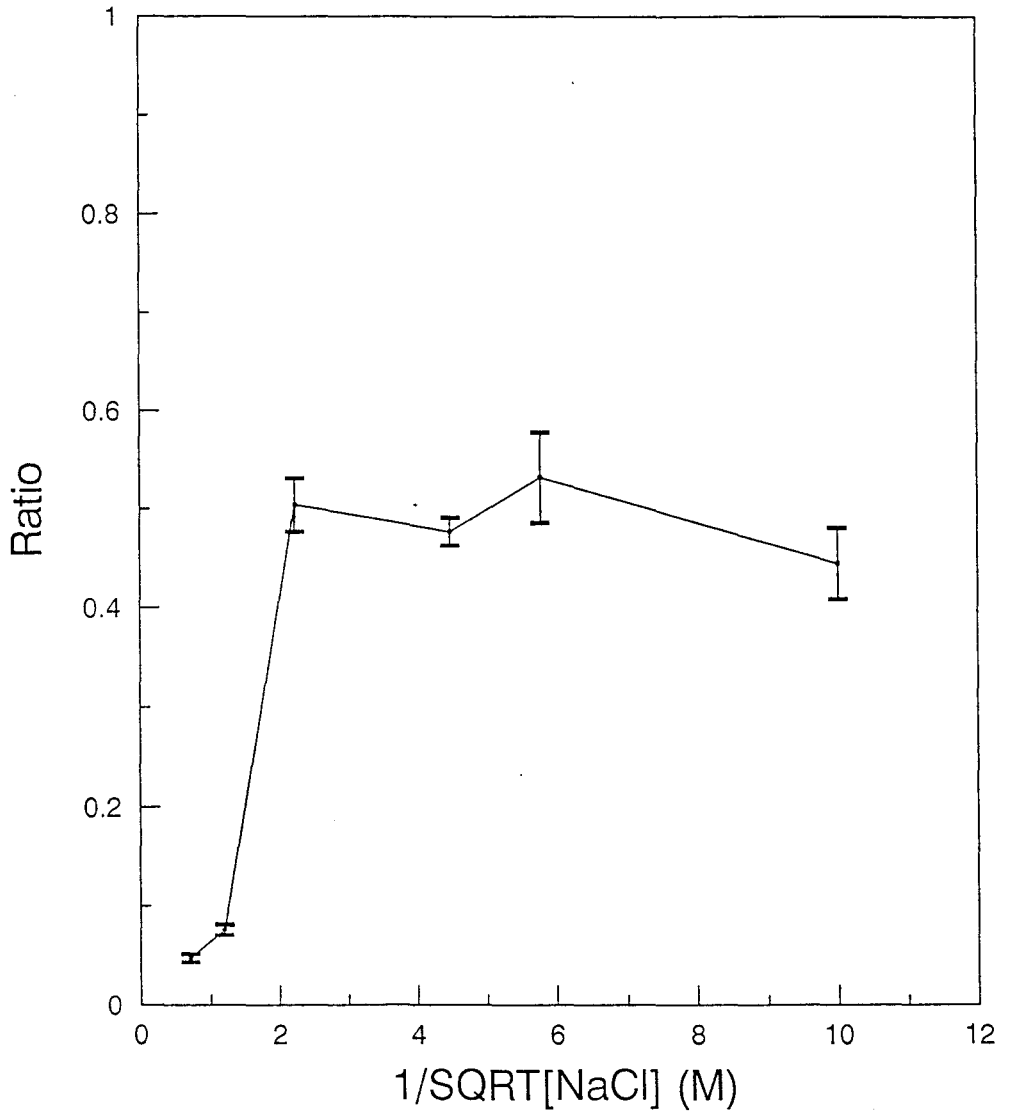


**TABLE 9 Effects of  $\text{Na}_3[\text{Fe}(\text{CN})_6]$  and  $\text{Na}_4[\text{Fe}(\text{CN})_6]$  Probes**

---

<u><math>1/\text{SQRT} [\text{NaCl}] (\text{M}^{-1/2})</math></u>	<u>Ratio (<math>\text{Na}_3[\text{Fe}(\text{CN})_6]</math>)</u>	<u>Ratio (<math>\text{Na}_4[\text{Fe}(\text{CN})_6]</math>)</u>
0.707	$0.013 \pm 0$	$0.047 \pm 0.004$
1.195	$0.056 \pm 0.001$	$0.076 \pm 0.005$
2.236	$0.43 \pm 0.008$	$0.504 \pm 0.027$
4.472	$0.585 \pm 0.003$	$0.477 \pm 0.014$
5.774	$0.556 \pm 0.019$	$0.532 \pm 0.046$
7.071	$0.593 \pm 0.01$	
10	$0.575 \pm 0.009$	$0.445 \pm 0.036$

---

## **6. Effect of NaCl Concentration on SWy-1 (reduced form)**

In order to compare charge effect on SWy-1 clay swelling, SWy-1 clay is reduced to its reduced form creating greater crystal charge. If all  $\text{Fe}^{3+}$  is reduced to  $\text{Fe}^{2+}$  in SWy-1 octahedral layer then the total charge per unit cell will increase to 1.0 esu/unit (see **Table 1**). We expect that this larger charged clay should play a role in the swelling of the clay beds as Schultz (12) and Horvath and Novak (13) claimed. Series of NaCl are used as electrolyte. **Table 10** and **Fig. 12** show the data of NaCl concentration effect on the reduced-form SWy-1 clay. The ratio data behaves similar to the regular SWy-1 results (**Fig. 8**). In both cases, a large increase in ratio occurs at  $[\text{Na}^+]^{-1/2}$  of 1.2 and a maximum ratio of 0.6 to 0.7 at  $[\text{Na}^+]^{-1/2}$  of 10 is obtained. This suggests that the more negatively charged clay behaves similarly to the less negatively charged clay, indicating that swelling does not depend upon charge but upon hydration effects for SWy-1 clay.

### **III. Studies on SAz-1 Clay**

#### **1. Effect of NaCl, KCl and $\text{CaCl}_2$ Concentration on the Swelling of SAz-1 ( $\text{Ca}^{2+}$ -form)**

A second comparison of charge effects was obtained by comparing oxidized SWy-1 (76.4 meq/100g) to oxidized SAz-1 (120.0 meq/100g) (See **Table 1**). The swelling behavior of Ca SAz-1 was obtained in various concentrations of NaCl, KCl and  $\text{CaCl}_2$ . **Fig. 13, 14** and **15** shows the data from NaCl, KCl, and  $\text{CaCl}_2$ , respectively. **Table 11** lists the data plotted in **Fig. 13, 14**, and **15**. The clay film never completely collapses in either high NaCl,  $\text{CaCl}_2$  or KCl electrolyte, contrary

**Fig. 12 A plot of ratio vs.  $1/\text{SQRT}[\text{NaCl}]$  obtained for 4 mM  $\text{K}_3[\text{Fe}(\text{CN})_6]$  at  $1 \mu\text{l}$  35 g/l reduced SWy-1 SPCME.**

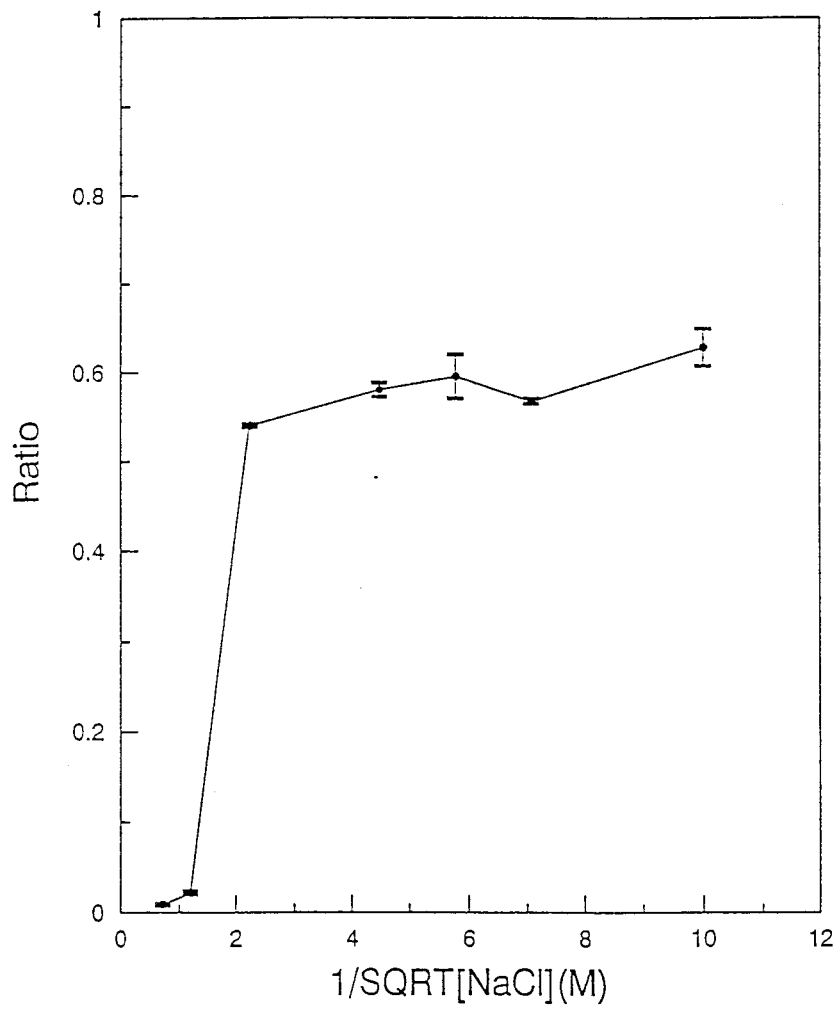


**TABLE 10 [NaCl] effect on reduced SWy-1**

---

<u>1/SQRT[NaCl] (M<sup>-1/2</sup>)</u>	<u>Ratio</u>
0.707	0.009 ± 0.001
1.195	0.022 ± 0.002
2.236	0.540 ± 0.002
4.472	0.580 ± 0.008
5.774	0.595 ± 0.025
7.071	0.567 ± 0.003
10	0.628 ± 0.021

---

**Fig. 13 A plot of ratio vs.  $1/\text{SQRT}[\text{NaCl}]$  obtained at  $1 \mu\text{l}$   $35 \text{ g/l}$  SAz-1 SPCME for  $4 \text{ mM}$   $\text{K}_3[\text{Fe}(\text{CN})_6]$**



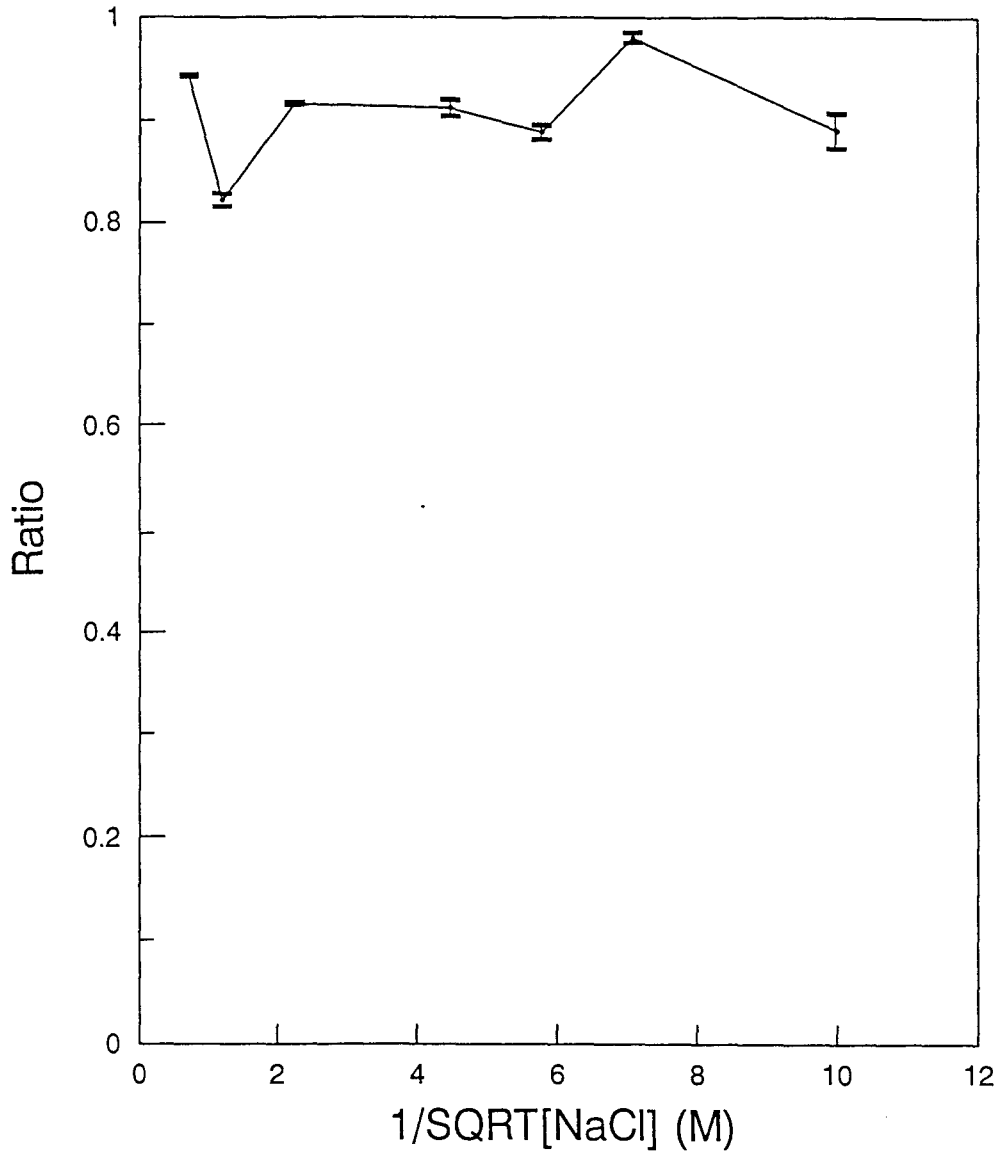


**Fig. 14 A plot of ratio vs.  $1/\text{SQRT}[\text{KCl}]$  obtained at  $1 \mu\text{l}$   $35 \text{ g/l}$  SAz-1 SPCME for  $4 \text{ mM}$   $\text{K}_3[\text{Fe}(\text{CN})_6]$  probe.**

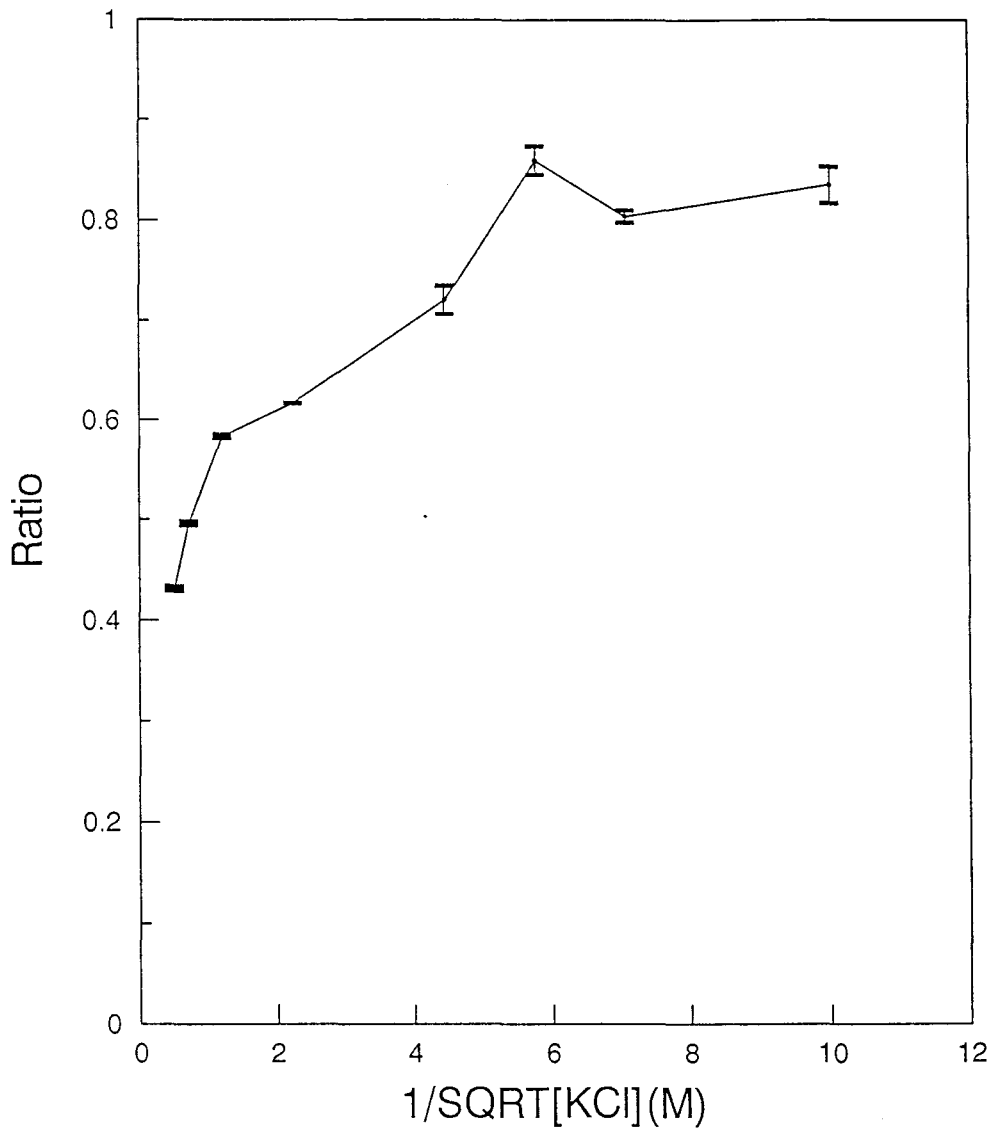


**Fig. 15** A plot of ratio vs.  $1/\text{SQRT}[\text{CaCl}_2]$  obtained at  $1 \mu\text{l}$   $35 \text{ g/l}$  SAz-1 SPCME for  $4 \text{ mM}$   $\text{K}_3[\text{Fe}(\text{CN})_6]$  probe.

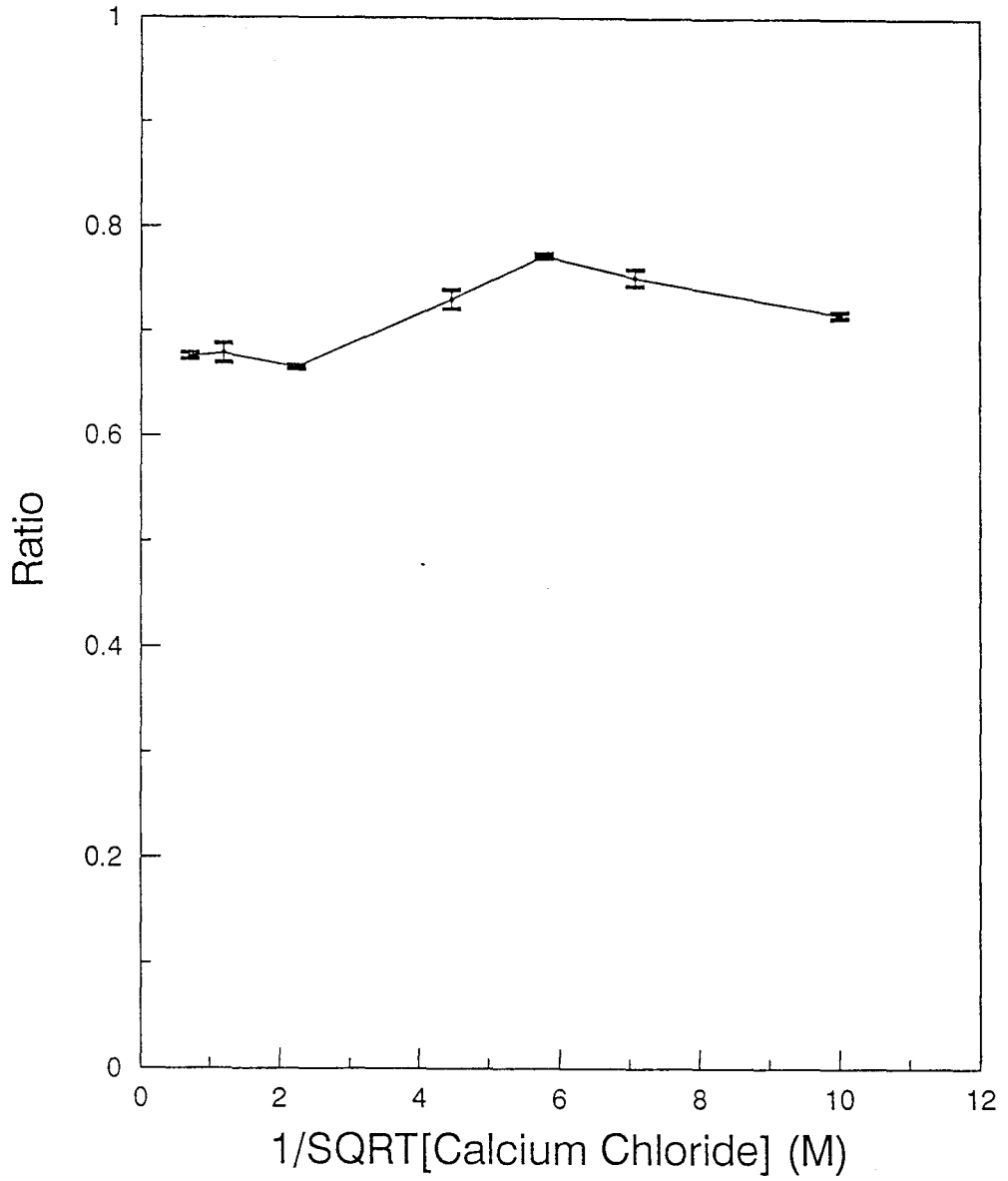


TABLE 11 [NaCl], [KCl], [CaCl<sub>2</sub>] effect on SAZ-1 (Note: X= NaCl, KCl, CaCl<sub>2</sub>)

---

<u>1/SQRT [X] (M)</u>	<u>Ratio(NaCl)</u>	<u>Ratio(KCl)</u>	<u>Ratio(CaCl<sub>2</sub>)</u>
0.5	0.431 ± 0.002		
0.707	0.942 ± 0.001	0.496 ± 0.002	0.676 ± 0.003
1.195	0.821 ± 0.006	0.584 ± 0.002	0.679 ± 0.009
2.236	0.915 ± 0.001	0.617 ± 0	0.666 ± 0.002
4.472	0.911 ± 0.008	0.721 ± 0.014	0.731 ± 0.009
5.774	0.887 ± 0.007	0.859 ± 0.014	0.773 ± 0.002
7.071	0.980 ± 0.005	0.804 ± 0.006	0.752 ± 0.008
10	0.889 ± 0.017	0.835 ± 0.018	0.716 ± 0.003

---

to our expectations, given the SWy-1 data. The electrical double layer theory is not applicable here. This is either because the SAz-1 (Ca<sup>+</sup> form) clay is highly disordered, e.g. containing lots of impurities (46) or because the Ca<sup>2+</sup> is never fully exchanged by K<sup>+</sup> or Na<sup>+</sup>, therefore never allowing a transition to a completely dehydrated state.

## **2.Effect of NaCl and KCl Concentration on the Swelling of SAz-1 (Na<sup>+</sup>-exchanged form)**

In order to remove the effect of the Ca<sup>2+</sup> cation and to make a better comparison to Na SWy-1 clay, SAz-1 (Ca form) was exchanged to its Na<sup>+</sup> form. The results of NaCl and KCl concentration effect on the SAz-1 (Na<sup>+</sup>-exchanged form) are expressed graphically in **Fig. 16** and **Fig. 17**, respectively. **Table 12** listed data from both **Fig. 16** and **Fig. 17**. These results show that the Na<sup>+</sup>-exchanged form of SAz-1 clay does collapse in high NaCl and high KCl concentrations. By comparing the SAz-1(Na<sup>+</sup>-exchanged form, CEC: ca. 120 meq/100g) (**Fig. 16**) vs SWy-1 (CEC: ca. 74 meq/100g) (**Fig. 9**), we find that the transition to a more porous film occurs at a higher electrolyte concentration ( $[\text{Na}^+]^{-1/2} < 1$  for SAz-1 and  $[\text{Na}^+]^{-1/2} > 1$  for SWy-1) for the more highly charged clay (SAz-1), suggesting that the amount of charge difference in the octahedral layer (see the charge distribution data in section II in Chapter I) may play a role in forcing the platelets apart from clay to clay. This is contrast to the charge comparison between SWy-1 and reduced form SWy-1. Also we find that the overall ratio in the expanded form for SAz-1 (Na<sup>+</sup>-exchanged form) is higher than the ratio

**Fig. 16 A plot of ratio vs.  $1/\text{SQRT}[\text{NaCl}]$  obtained at  $1 \mu\text{l}$   $35 \text{ g/l}$  SAz-1 ( $\text{Na}^+$ -exchanged form) SPCME for  $4 \text{ mM}$   $\text{K}_3[\text{Fe}(\text{CN})_6]$  probe.**



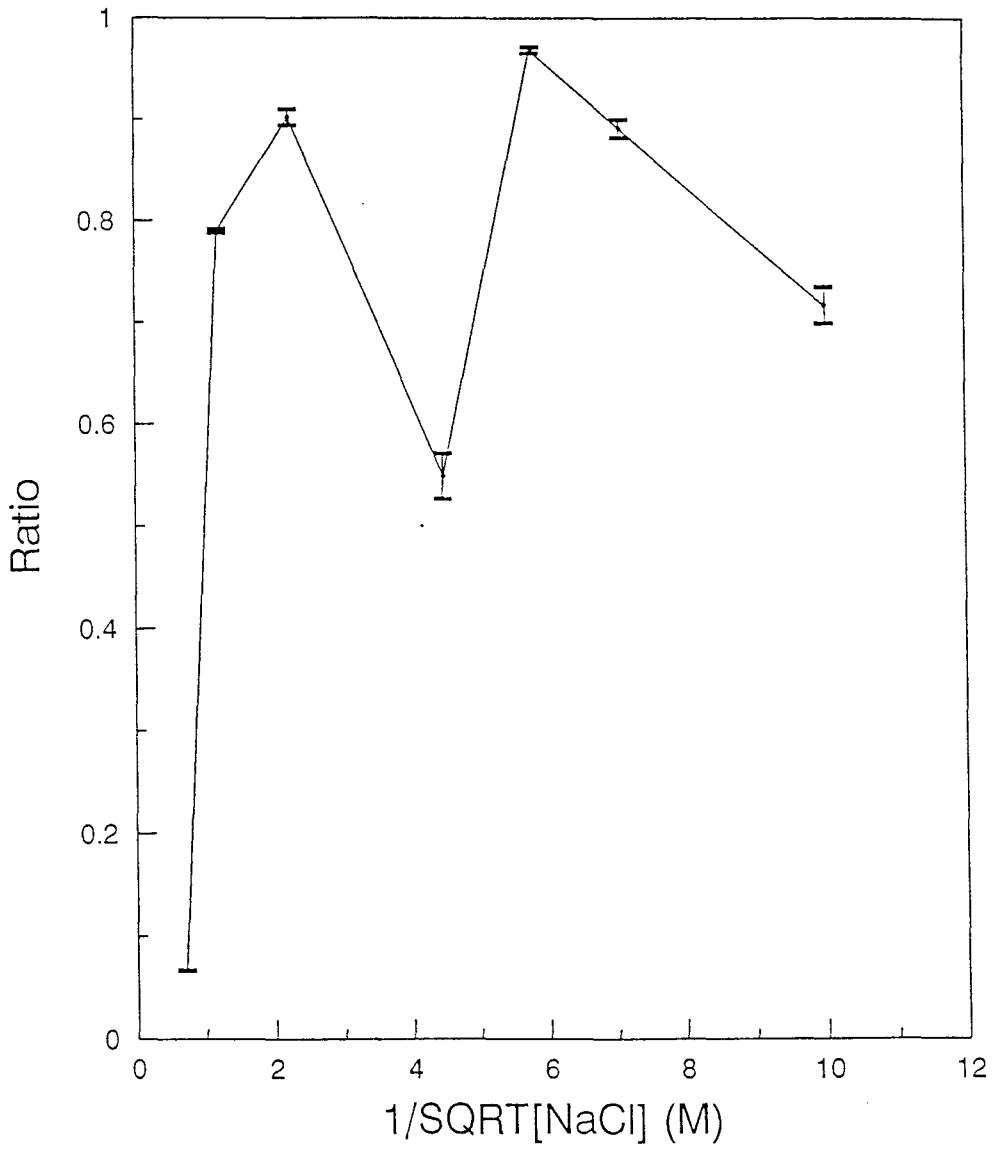


**Fig. 17 A plot of ratio vs.  $1/\text{SQRT}[\text{KCl}]$  obtained at  $1 \mu\text{l}$   $35 \text{ g/l}$  SAz-1( $\text{Na}^+$ -exchanged form) SPCME for  $4 \text{ mM}$   $\text{K}_3[\text{Fe}(\text{CN})_6]$  probe.**

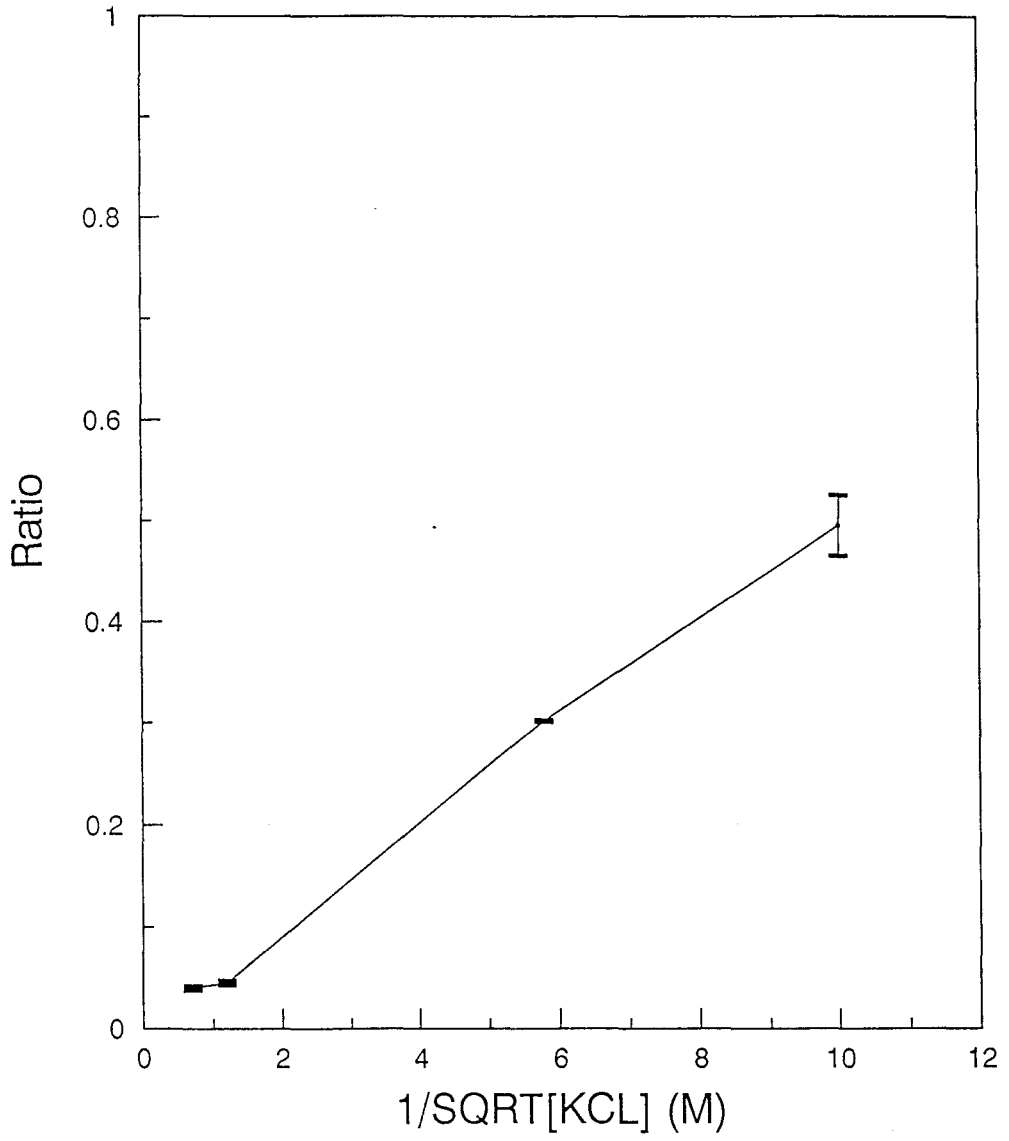


**Table 12 [NaCl], [KCl] Effect on SAz-1 (Na<sup>+</sup>-exchange form)**

---

<u>1/SQRT [NaCl] and [KCl] (M<sup>-1/2</sup>)</u>	<u>Ratio (NaCl)</u>	<u>Ratio (KCl)</u>
0.707	0.067 ± 0.001	0.040 ± 0.002
1.195	0.790 ± 0.002	0.045 ± 0.002
2.236	0.902 ± 0.0082	
4.472	0.549 ± 0.022	
5.774	0.968 ± 0.003	0.302 ± 0.001
7.071	0.891 ± 0.009	
10	0.717 ± 0.018	0.495 ± 0.03

---

for the expanded SWy-1 clay film, again suggesting that the amount of charge difference in the octahedral layer may play a role in the swelling process of SAz-1 clay.

#### **IV. Summary and Future Direction**

A relatively simple and easy electrochemical method (CME) was used to study the clay swelling. Two different charged clays, SWy-1 and SAz-1, were studied by changing the probes and the electrolytes. Several methodology related preliminary questions were straightened out. SEM confirmed the homogeneous coverage of clay on the electrode. Soaking time experiments verified the SPCME stability. The scan rate dependence experiment allowed an optimum scan rate of 50 mv/s to be chosen by which the diffusion layer would reside within the clay film.

The results of NaCl, KCl, and CaCl<sub>2</sub> concentration effects on the swelling of SAz-1 (Ca form) clay showed that the clay film never completely collapsed in these electrolytes. We attributed this to either highly disordered SAz-1 (Ca form) clay (e.g. containing lots of impurities) or that the Ca<sup>2+</sup> is never fully exchanged by K<sup>+</sup> or Na<sup>+</sup>. Our results are inconclusive with respect to the effect of clay charge on swelling. On the one hand, the more highly charged SAz-1 (Na form) showed that it did collapse under the condition of higher NaCl or KCl concentrations than necessary for the SWy-1 clays. On the other hand, the more highly charged reduced SWy-1 clay showed no difference in its swelling behavior from the lower charged SWy-1 clay. From the formulae we could roughly estimate that the total charge of these two clays was nearly equal. Therefore, we assumed that charge

was not a variable here. We suggested that the different behavior might be due to the difference of the amount of  $Mg^{2+}$  and  $Fe^{3+}$  between the reduced SWy-1 clay and the  $Na^+$ -exchanged SAz-1 clay. This could cause different crystal dimension affects close range interaction of hydrated cations effect, thus changing the swelling behavior.

The results of different charge probe studies for SWy-1 clay showed that the higher negative charge probe was excluded from the film more easily than the lower negative charge probe. This was in line with our expectation since the clay was negatively charged layers. The results also showed that if the cation from the probe molecule was different from the cation form of the exchanged clay, it might promote heterogeneity from sample to sample or cause the multiple layer effect. The results of NaCl concentration effect suggested that the swelling process of SWy-1 clay was a step-wise expansion rather than the linear expansion observed by Norrish's X-ray diffraction results and by Lee's oven-dried CME results in the low concentration region.

In the future, we ought to further conduct our charge effect studies. This could include the experiments such as KCl and  $CaCl_2$  concentration effects on the reduced SWy-1 clay, different probes' effects on SAz-1 clay (both Ca form and Na form), etc. Besides, the divalent and trivalent electrolyte effects on both clays needed to be understood. In these experiments, we wish to add some of the environmentally important toxic inorganic or organic compounds to our clay diffusion studies. In the mean time, we would like to perform low angle X-ray diffraction in an environmental chamber so that the electrolyte would not be dried

out and the humidity could also be controlled. We hope that we will obtain results similar to our CME methods.

## BIBLIOGRAPHY

1. Laszlo, P.; *Science*, **1987**, *235*, 1473.
2. A Review Article by Bard, A.J.; "*Electrodes Modified with Clays, Zeolites and Related Microporous Solids*", in preparation
3. van Olphen, H.; "*An Introduction to Clay Colloid Chemistry*", Wiley, New York, **1977**.
4. Brindley, G.W.; Brawn, G., eds.; "*Crystal Structures of Clay Minerals and their X-Ray Diffraction*", Mineral Soc., Monogr.5: London, **1980**.
5. Hiroshi, I.; *J. Electroanal. Chem.*, **1988**, *249*, pp. 133-134
6. Newman, A.C.; "*Chemistry of Clays and Clay Mineral*", Mineralogical Society Monograph 7, Wiley, New York, **1987**, pp. 48-61
7. Sato, T.; Watanabe, T. and Otsuka R.; *Clays and Clay Minerals*, **1992**, *40*, pp. 103-113.
8. van Olphen, H.; Fripiat, J.J.; "*Data Handbook for Clay Materials and other Non-Metallic Minerals*", Pergamon Press, New York, **1979**.
9. Lee, J.F.; Mortland, M.M. and Chiou, C.T.; *Clays and Clay Minerals*, **1990**, *38*, pp.113-120



10. Norrish, K.; Quirk, J.P.; *Nature*, **1954**, *173*, pp. 255-256
11. Cody, R.D.; Thompson, G.L.; *Clays and Clay Minerals*, **1976**, *24*, pp. 224-231
12. Schultz, L. G.; *Clays and Clay Minerals*, **1969**, *17*, pp. 115-149
13. Horvath, I.; Novak, I.; Proc. Int. *Clay Conf., Mexico City*, **1975**, S.W.Bailey, ed., pp. 185-189
14. Bard A.J. and Faulkner, L.R.; "*Electrochemical Methods : Fundamentals and Applications*", Wiley, New York, **1988**.
15. Evans, H.D.; *J. Chemical Education*, **1983**, *60*, 290.
16. Wang, J.; "*Electroanalytical Techniques in Clinical Chemistry and Laboratory Medicine*", VCH, New York, **1988**.
17. Rieger, P.H.; "*Electrochemistry*", Prentice-Hall, New Jersey, **1987**.
18. Marshall, C.E.; *J. Phys. Chem.*, **1939**, *43*, 1155.
19. Fitch, A.; "*Use of Clay Modified Electrode in Pollution Transport Problems*", in preparation.
20. Murry, R.W. and Bard, A.J., ed.; *J. Electroanal. Chem.*, **1984**, Vol.13, Dekker, New York, pp. 191.
21. Oyama, N. and Anson, F.C.; *J. Electroanal. Chem.*, **1986**, *199*, pp. 467-470.
22. Rusling, J.F.; Shi, C.N. and Suib, S.L.; *J. Electroanal. Chem.*, **1988**, *245*, pp. 331-337.
23. White, J.R. and Bard, A.J.; *J. Electroanal. Chem.*, **1986**, *197*, pp. 233-244.
24. Castro-Acuna, C.M.; Fan, F.R.F. and Bard, A.J.; *J. Electroanal. Chem.*,

- 1987**, 234, pp.347-353.
25. Ghosh, P.K.; Mau, A.W.H. and Bard, A.J.; *J. Electroanal. Chem.*, **1984**, 169, pp. 315-317.
  26. Inoue, H. and Yoneyama, H.; *J. Electroanal. Chem.*, **1987**, 233, pp. 291-294.
  27. Inoue, H.; Haga, S.; Iwakura, C. and Yoneyama, H.; *J. Electroanal. Chem.*, **1988**, 249, pp. 133-141.
  28. Itaya, K. and Bard, A.J.; *J. Phys. Chem.*, **1985**, 89, pp. 5565-5568.
  29. Itaya, K.; Chang, H.C. and Uchida, I.; *Inorg. Chem.*, **1987**, 26, 624.
  30. Kamat, P.V.; *J. Electroanal. Chem.*, **1984**, 163, pp. 389-394.
  31. "Purification of Laboratory Chemicals", 3 rd edition, Pergamon Press, New York, **1988**.
  32. Norrish, K.; *Trans. Farad. Soc.*, **1954**, 18, pp. 120-134.
  33. Gibbs, R.J.; *Am. Mineral.*, **1941**, 50, 1965.
  34. Norrish, K. and Rausell-Colom, J.A.; *Clays and Clay Minerals*, **1963**, 10, 123.
  35. Viani, B.E.; Low, P.F. and Roth, C.B.; *J. Coll. Interf. Sci.*, **1983**, 96, 229.
  36. Van der Gast and Jansen, J.H.F.; *Clays and Clay Minerals*, **1985**, 33, 5, 472
  37. Simonton, T.C.; *Clays and Clay Minerals*, **1985**, 33, 472
  38. Brindley, G.W. and Simonton, T.C.; *Clays and Clay Minerals*, **1984**, 32, pp. 235-237.
  39. Mahra, O.P. and Jackson, M.L.; *Clays and Clay Minerals*, **1960**, 7, 317.

40. Stucki, J.W.; *Clays and Clay Minerals*, **1984**, 32, 350.
41. King, R.D.; Nocera, D.G. and Pinnavaia, T.J.; *J. Electroanal. Chem.*, **1987**, 236, 48.
42. Fitch, A. and Du, J.; *J. Electroanal. Chem.*, **1991**, 319, pp. 409-414.
43. Lee, S.A. and Fitch, A.; *J. Phys. Chem.*, **1990**, 94, 12, pp. 4998-5004.
44. Tokuda, A.; Morita, K. and Shimizu, Y.; *Anal. Chem.*, **1989**, 61, 1763.
45. Fitch, A.; *J. Electroanal. Chem.*, submitted.
46. Guven, N.; *Clays and Clay Minerals*, **1974**, 22, pp. 155-156.

## VITA

The author, Jia Du, was born in May 6, 1963 in Shanghai, China.

In September, 1982, he entered Shanghai University of Technology and received the Bachelor Degree of Science with a major in Chemistry in July, 1986. During September 1986 to June 1989, he was working as a Research Assistant at the Institute of Microbiology, Chinese Academy of Science, Beijing, China.

In September 1989, Jia Du joined Department of Chemistry at Loyola University of Chicago to pursue graduate studies in chemistry. He was awarded a teaching assistantship from September 1989 to August 1991. He was also supported by a research assistantship as part of the research grant awarded to Dr. Alanah Fitch by the National Science Foundation from September 1991 to September 1992.

## APPROVAL SHEET

The thesis submitted by Jia Du has been approved by the following committee:

Dr. Alanah Fitch, Director

Associate Professor of Chemistry, Loyola

Dr. Albert Herlinger

Associate Professor of Chemistry, Loyola

Dr. David Crumrine

Associate Professor of Chemistry, Loyola

The final copies have been examined by the director of the thesis and the signature which appears below verifies the fact that any necessary changes have been incorporated and that the thesis is now given final approval by the Committee with reference to content and form.

The thesis is, therefore, accepted in partial fulfillment of the requirements for the degree of Master of Science.

12/9/92

Date

Alanah Fitch

Director's Signature